

# DIS structure functions and the double-spin asymmetry in $\rho^0$ electroproduction within a Regge approach

N.I. Kochelev\*

*Bogoliubov Laboratory of Theoretical Physics, JINR, Dubna, Moscow region, 141980 Russia<sup>†</sup>*

K. Lipka<sup>‡</sup> and W.-D. Nowak<sup>§</sup>  
*DESY Zeuthen, 15738 Zeuthen, Germany*

V. Vento<sup>¶</sup>

*Departament de Física Teòrica and Institut de Física Corpuscular,  
Universitat de València-CSIC E-46100, Burjassot (Valencia), Spain*

A.V. Vinnikov\*\*

*Bogoliubov Laboratory of Theoretical Physics, JINR, Dubna, Moscow region, 141980 Russia<sup>††</sup>*

(Dated: December 31, 2013)

The proton, neutron and deuteron structure functions  $F_2(x, Q^2)$  and  $g_1(x, Q^2)$ , measured at intermediate  $Q^2$ , are analyzed within a Regge approach. This analysis serves to fix the parameters of this scheme which are then used to calculate, in a unified Regge approach, the properties of  $\rho^0$  meson electroproduction on the proton and the deuteron. In this way, the double-spin asymmetry observed at HERMES in  $\rho^0$  electroproduction on the proton, can be related to the anomalous behavior of the flavor-singlet part of the spin-dependent structure function  $g_1(x, Q^2)$  at small  $x$ .

PACS numbers: 12.40.Nn, 13.60.Le, 13.75.Cs, 13.88.+e

## I. INTRODUCTION

Understanding the spin structure of the nucleon is today one of the main problems in hadron physics. Polarized beams have allowed significant progress in the measurement of the nucleon spin-dependent structure functions in the Deep Inelastic Scattering (DIS) regime. A result of some of these measurements [1] is that, at small values of Björken  $x$ , the neutron spin-dependent structure function  $g_1^n(x, Q^2)$ , which according to the  $SU(6)_W$  model is dominated by the flavor singlet quark sea part, exhibits an anomalous behavior. More precisely, at  $x \rightarrow 0$ ,  $g_1^n(x, Q^2) \sim 1/x$ , while the expected behavior should be  $1/x^{\alpha_{a_1}}$ , where  $a_1$  is a conventional Regge trajectory with appropriate quantum numbers and intercept  $\alpha_{a_1} = -0.5 \div 0.5$ . Experimental data are thus well described in terms of a leading trajectory with an intercept close to 1, a value reminiscent of the Pomeron. In fact, this type of behavior at small  $x$  was predicted by leading order perturbative QCD calculations [2]. However, since next-to-leading order corrections to the perturbative BFKL Pomeron [3] are large [4], it is not clear to

which extent the perturbative description is valid.

In Ref. [5], the observed anomalous behavior of  $g_1^n(x, Q^2)$ , was assumed to signal the existence of a flavor-singlet exchange with large intercept and negative signature, which was then used to explain the experimental data on diffractive hadronic reactions: vector meson photoproduction at  $\sqrt{s} \approx 100$  GeV,  $|t|=1 \div 10$  GeV<sup>2</sup> and proton-proton elastic scattering at  $\sqrt{s}=20 \div 60$  GeV,  $|t|=2 \div 10$  GeV<sup>2</sup> [5, 6]. This exchange gives sizeable contributions to the differential cross-sections at large energy due to the large value of its intercept. We called it  $f_1$  since its quantum numbers coincide with those of the axial vector  $f_1(1285)$  meson ( $P=C=+1$ , negative signature). The mechanism leading to this exchange in QCD is not known. The relation of the Pomeron with the scale anomaly, led us to conjecture a relation between the  $f_1$  and the gluonic axial anomaly, since the  $f_1$  strongly mixes with gluonic degrees of freedom [5].

In order to investigate this unnatural-parity exchange the best observables are spin-dependent cross-sections. For example, we already have shown that the  $f_1$  exchange leads to large double-spin asymmetries in different diffractive reactions [5, 7, 8].

For  $s$ -channel helicity conserving (SCHC) reactions it seems reasonable, in the context of the VMD model, to establish a relation between the matrix elements describing the structure functions and vector meson electroproduction at low  $-t$ , as indicated in Fig. 1. This relation arises naturally in the context of the Regge approach [9], where the imaginary part of the forward Compton scattering amplitude, relevant to describe DIS structure functions, and the total amplitude for vector meson production at  $-t \rightarrow 0$  are connected.

\*Electronic address: kochelev@thsun1.jinr.ru

<sup>†</sup>Also at Institute of Physics and Technology, Almaty, 480082, Kazakhstan

<sup>‡</sup>Electronic address: Katerina.Lipka@desy.de

<sup>§</sup>Electronic address: Wolf.Dieter.Nowak@desy.de

<sup>¶</sup>Electronic address: vicente.vento@uv.es

\*\*Electronic address: vinnikov@thsun1.jinr.ru

<sup>††</sup>Also at School of Physics, Seoul National University, Seoul 151-747, Korea

The Regge model is a well known approach to describe diffractive reactions with small momentum transfer and high energy, a kinematic region where non-perturbative QCD effects are important. For this reason the investigation of diffraction and structure functions at low  $x$  are important items included into the experimental programs of the current and future accelerators: HERA, TEVATRON, RHIC, LHC, etc. These studies are expected to considerably enlarge the insight into the nature of strong interactions between quarks at large distances [10]. Several scenarios for the direct relation between the complex structure of the QCD vacuum and Regge behavior have been suggested [11, 12, 13].

The effective propagator for the spin-nonflip amplitude for scattering of two particles with momenta  $p_1$  and  $p_2$  has the following form in Regge theory:

$$D_R(s, t) = -\frac{1}{\sin(\pi\alpha_R(t))\Gamma(\alpha_R(t))} \left(\frac{s}{s_0}\right)^{\alpha_R(t)-1} \times \\ \times \left[1 + \sigma_R \cos(\pi\alpha_R(t)) - \iota \cdot \sigma_R \sin(\pi\alpha_R(t))\right], \quad (1)$$

where  $s = (p_1 + p_2)^2$ ,  $t = (p_1 - p_2)^2$ ,  $s_0$  is  $\max(p_1^2, p_2^2, p_1'^2, p_2'^2)$ ,  $\alpha_R(t)$  describes the Regge trajectory of the particles exchanged in the  $t$  channel and  $\sigma_R$  their signature, related to the spin  $J$  by  $\sigma = (-1)^J$ . The  $\Gamma$  function in the denominator provides the correct analytic behavior of the amplitude [14]. In many cases, a simpler formula can be used [15], but we prefer the original form in order to keep a precise relation between the real and the imaginary parts of the amplitude. This relation will be used below to establish a connection between the properties of the DIS structure functions and those of vector meson electroproduction off the nucleon as suggested above.

Reggeons, with signature and space parities of the same sign,  $\sigma = P$  (natural parity), have an amplitude which does not depend on the helicities of the colliding particles. Their exchange gives the dominant contributions to the spin-independent nucleon structure functions and to the total cross-sections. Exchanges with unnatural parity,  $\sigma = -P$ , have an amplitude which is proportional to the product of the particle helicities. Thus, only Reggeons with unnatural parities can contribute to the spin-dependent structure function  $g_1(x, Q^2)$ . Furthermore, a longitudinal double-spin asymmetry in two-particle scattering only arises when an unnatural-parity-exchange contribution to the scattering amplitude exists.

The main goal of this paper is an analysis of the deep-inelastic structure functions  $F_2(x, Q^2)$  and  $g_1(x, Q^2)$  in the framework of the Regge model; the extracted Reggeon parameters will be used to calculate the elastic cross-section, and finally the double-spin asymmetry, of  $\rho^0$  electroproduction for intermediate values of  $Q^2$ .

The Regge scheme will be defined by the exchange of trajectories with very large intercepts (Pomeron and the ‘anomalous’ component of  $f_1$ ) and of secondary Regge trajectories, namely  $f_2$ ,  $a_2$ , the ‘normal’ component of

$f_1$  (which will be called  $f_1'$ ) and  $a_1$ . Especially the contributions of secondary Reggeons are considered to be of importance at HERMES energies,  $\sqrt{s} = 7$  GeV.

## II. THE STRUCTURE FUNCTION $F_2(x, Q^2)$ IN A REGGE APPROACH AT INTERMEDIATE VALUES OF $Q^2$

The parameters of the natural-parity Reggeons in soft interactions ( $Q^2 < 1$  GeV<sup>2</sup>) are quite well known. They can be obtained from fits to the total hadronic cross-sections [16]. In particular, the parameters of the Pomeron,  $f_2$  and  $a_2$  Reggeon trajectories which are relevant for our calculation, are given by the Particle Data Group [17]:

$$\alpha_P(t) = 1.093 + 0.25 t, \beta_{Pqq} = \beta_{PNN}/3 = 1.6 \text{ GeV}^{-1}, \\ \alpha_{f_2}(t) = 0.358 + 0.9 t, \beta_{f_2qq} = \beta_{f_2NN}/3 = 4.7 \text{ GeV}^{-1}, \\ \alpha_{a_2}(t) = 0.545 + 0.9 t, \beta_{a_2qq} = \beta_{a_2NN} = 4.9 \text{ GeV}^{-1}, \quad (2)$$

where  $\beta_{RNN}$  and  $\beta_{Rqq}$  are the coupling constants for the Reggeon-nucleon and Reggeon-quark couplings, respectively. The effective Lorentz structure of the coupling of these Reggeons to nucleons and quarks is assumed to be  $\gamma_\mu$  [18]. The values of the slopes of the trajectories, which cannot be obtained from a fit to the total hadronic cross-sections, are taken from Ref. [9]. The relation between the couplings to quarks and nucleons is obtained from the naive constituent quark model. A clear separation of the secondary Reggeons and the Pomeron is possible because the energy dependencies of their amplitudes described by the intercepts  $\alpha(0)$ ,  $\sigma_R^{tot} \sim s^{\alpha_R(0)-1}$  are very different. Specifically, the Pomeron contribution to the total hadronic cross-section rises as  $s^{0.093}$ , while, for example, the  $f_2$  contribution falls as  $s^{-0.642}$ .

For large virtualities of the scattering particles, the effective intercepts of the Pomeron and the Reggeons change [19]. In particular, it was measured by the H1 and ZEUS Collaborations at HERA [20, 21] that the effective Pomeron intercept, extracted from the analysis of the  $F_2(x, Q^2)$  structure function, ranges from about 1.1 at  $Q^2 \approx 0$  to about 1.4 at  $Q^2 > 10^2$  GeV<sup>2</sup>. Therefore, to make predictions for HERMES ( $< Q^2 > = 1.7$  GeV<sup>2</sup>), knowledge of the Pomeron and Reggeons intercepts at  $Q^2$  values of a few GeV<sup>2</sup> is required.

The Regge formulae [22] for the proton and deuteron structure functions used are

$$F_2^p(x, Q^2) = \frac{Q^2}{Q^2 + \mu_N^2} \times \\ \times \left( \frac{A_P}{x^{\alpha_P(0)-1}} + \frac{A_{f_2}}{x^{\alpha_{f_2}(0)-1}} + \frac{A_{a_2}}{x^{\alpha_{a_2}(0)-1}} \right), \\ F_2^d(x, Q^2) = \frac{Q^2}{Q^2 + \mu_N^2} \left( \frac{A_P}{x^{\alpha_P(0)-1}} + \frac{A_{f_2}}{x^{\alpha_{f_2}(0)-1}} \right). \quad (3)$$

The various structure functions appearing in these equations represent the  $SU(3)_f$  flavor singlet (the Pomeron),

the  $SU(2)_f$  isoscalar ( $f_2$ ) and the isovector ( $a_2$ ) exchanges. The parameter  $\mu_N$  effectively accounts for the scaling violation at small  $Q^2$  for the natural parity exchanges. Using Eq. (3) we made a fit (not shown) to the recent  $F_2$  data [23] at  $Q^2 = 1 \div 3 \text{ GeV}^2$  and  $x \lesssim 0.1$  (Regge region). The extracted parameters of Pomeron,  $f_2$  and  $a_2$  Reggeons are

$$\begin{aligned} A_P &= 0.15 \pm 0.02, & \alpha_P(0) &= 1.20 \pm 0.01; \\ A_{f_2} &= 0.46 \pm 0.05, & \alpha_{f_2}(0) &= 0.61 \pm 0.07; \\ A_{a_2} &= 0.12 \pm 0.11, & \alpha_{a_2}(0) &= 0.36 \pm 0.28; \\ & & \mu_N &= 0.80 \pm 0.02 \text{ GeV}. \end{aligned} \quad (4)$$

This fit provides a value of  $\chi^2 = 191.2$  for 164 data points ( $\chi^2/\text{ndof}=1.17$ ). It is evident that already in the semi-hard region ( $Q^2$ -values of a few  $\text{GeV}^2$ ) modified Regge intercepts have to be used. The slopes can be assumed to remain unchanged as they seem to vary quite slowly in this  $Q^2$  region [26]. Moreover, they have no strong effect on the double-spin asymmetry.

### III. THE SPIN-DEPENDENT STRUCTURE FUNCTION $g_1(x, Q^2)$ IN A REGGE APPROACH.

Parameters for unnatural-parity Reggeons have been extracted earlier using Regge-type *phenomenological fits* to the spin-dependent structure function  $g_1(x, Q^2)$  [24, 25]. In our approach not only effective intercepts of Regge exchanges are determined, but also their couplings with nucleons and quarks. These couplings are a necessary input to the calculation of the double-spin asymmetry in vector meson electroproduction (see below). We use the relation between  $g_1(x, Q^2)$  and the imaginary part of the spin-dependent forward Compton scattering amplitude. By *direct calculation* (Fig. 1a) the contribution of the unnatural-parity-Reggeon exchanges to this amplitude is obtained as:

$$\begin{aligned} T^{\mu\nu}(q, p, S) &= \beta_{Rqq}\beta_{RNN}C_R\bar{u}(p, S)\gamma_\alpha\gamma_5 u(p, S) \times \\ &\times R^{\mu\nu\alpha} \frac{1 - \exp\{-i\pi\alpha_R(0)\}}{\sin\{\pi\alpha_R(0)\}\Gamma(\alpha_R(0))} \left(\frac{2p \cdot q}{s_0}\right)^{\alpha_R(0)-1}, \end{aligned} \quad (5)$$

where we assume that all exchanges  $f_1$ ,  $f'_1$  and  $a_1$  have a  $\gamma_\alpha\gamma_5$  Lorenz structure for both the quark and the nucleon vertices. The nucleon spin is denoted by  $S$ , and  $s_0 \approx Q^2$  is the characteristic scale in the process.

The factor  $C_R$  is given by  $e_u^2 + e_d^2 + e_s^2$  for the  $SU(3)_f$  singlet ‘anomalous’ exchange ( $f_1$ ), by  $e_u^2 + e_d^2$  for the  $SU(2)_f$  singlet ‘normal’ exchange ( $f'_1$ ) and by  $e_u^2 - e_d^2$  for the  $SU(2)_f$  triplet  $a_1$ ;  $R^{\mu\nu\alpha}$  is given by Ref. [27]

$$\begin{aligned} R^{\mu\nu\alpha} &= -2 \int \frac{d^4k}{(2\pi)^4} \frac{1}{(k^2 - m_q^2)((k - q)^2 - m_q^2)} \times \quad (6) \\ T_R[(m_q + \hat{k} + \hat{q})\gamma^\nu (m_q + \hat{k})\gamma^\nu (m_q + \hat{k} + \hat{q})\gamma^\alpha\gamma_5], \end{aligned}$$

where  $m_q$  is the mass of the quark in the quark loop in Fig. 1.

Using the relation  $\bar{u}(p, S)\gamma_\alpha\gamma_5 u(p, S) = 2mS_\alpha$ , and the formula

$$R^{\mu\nu\alpha} = \frac{1}{2\pi^2} q_\tau \epsilon^{\tau\mu\nu\alpha}, \quad (7)$$

for  $-q^2 \gg m_q^2$  [28] we have

$$\begin{aligned} T^{\mu\nu}(q, p, S) &= \frac{m}{\pi^2} C_R \beta_{Rqq} \beta_{RNN} S_\alpha q_\tau \epsilon^{\tau\mu\nu\alpha} \times \quad (8) \\ &\times \frac{1 - \exp\{-i\pi\alpha_R(0)\}}{\sin\{\pi\alpha_R(0)\}\Gamma(\alpha_R(0))} \left(\frac{2p \cdot q}{Q^2}\right)^{\alpha_R(0)-1}. \end{aligned}$$

This expression is compared to the general form

$$\begin{aligned} T_{(spin)}^{\mu\nu} &= i\epsilon^{\mu\nu\alpha\beta} q_\alpha S_\beta \frac{m}{pq} T_3 + \quad (9) \\ &+ i\epsilon^{\mu\nu\alpha\beta} q_\alpha (S_\beta (p \cdot q) - p_\beta (S \cdot q)) \frac{m}{(p \cdot q)^2} T_4, \end{aligned}$$

where the DIS structure functions  $g_1$  and  $g_2$  are related to the amplitudes  $T_3$ ,  $T_4$  by

$$g_1(q, \nu) = -\frac{\text{Im}(T_3)}{2\pi}, \quad g_2(q, \nu) = -\frac{\text{Im}(T_4)}{2\pi}, \quad (10)$$

and where  $\nu = p \cdot q$ .

By assuming that the structure function  $g_2$  is small, we obtain

$$g_1(q, \nu) = \frac{\nu C_R \beta_{Rqq} \beta_{RNN}}{2\pi^3 \Gamma(\alpha_R(0))} \left(\frac{\nu}{Q^2}\right)^{\alpha_R(0)-1} \quad (11)$$

Using  $x = Q^2/2\nu$  we have

$$g_1(x, Q^2) = \frac{C_R \beta_{Rqq} \beta_{RNN}}{4\pi^3 \Gamma(\alpha_R(0))} \frac{Q^2}{x^{\alpha_R(0)}}. \quad (12)$$

This form does not yet provide the correct scaling behavior for the structure function at  $Q^2 \rightarrow \infty$  since the non-locality of the Reggeon-quark vertex in Fig. 1a was not taken into account. Phenomenologically, this can be accomplished by introducing a form factor (as has been done in the Pomeron case [29]):

$$F(Q^2) = \frac{\mu_U^2}{Q^2 + \mu_U^2}, \quad (13)$$

where  $\mu_U$  is the effective parameter describing the scaling violation at low  $Q^2$  for the unnatural-parity Reggeons. Then the contribution of a Reggeon to the  $g_1(x, Q^2)$  structure function reads

$$g_1(x, Q^2) = \frac{\mu_U^2 C_R \beta_{Rqq} \beta_{RNN}}{4\pi^3 \Gamma(\alpha_R(0))} \frac{Q^2}{Q^2 + \mu_U^2} \frac{1}{x^{\alpha_R(0)}} \quad (14)$$

which provides the correct scaling behavior of the structure function at large  $Q^2$ .

The parameters of the Reggeons with unnatural parity can be found from a fit to the available data on polarized DIS. Since data exist for proton, neutron and deuteron

targets, this allows the separation of the isoscalar and isovector parts of the respective structure functions

$$\begin{aligned} g_1^p(x, Q^2) &= g_1^{(1)}(x, Q^2) + g_1^{(3)}(x, Q^2), \\ g_1^n(x, Q^2) &= g_1^{(1)}(x, Q^2) - g_1^{(3)}(x, Q^2), \\ g_1^d(x, Q^2) &= g_1^{(1)}(x, Q^2), \end{aligned} \quad (15)$$

where  $g_1^{(1)}(x, Q^2)$  and  $g_1^{(3)}(x, Q^2)$  are the isoscalar and isovector components, respectively.

It was pointed out [24] that the isoscalar part contains two components: ‘normal’ and ‘anomalous’. The ‘normal’ component has an intercept of  $\alpha(0) \approx 0.5$  while the ‘anomalous’ has a large intercept,  $\alpha(0)$  close to 1. Using Eq. (14), the structure functions in Eq. (15) can be written

$$\begin{aligned} g_1^{(1)}(x, Q^2) &= \frac{2\mu_U^2\beta_{f_1qq}\beta_{f_1NN}}{3\ 4\pi^3\Gamma(\alpha_{f_1}(0))} \frac{Q^2}{Q^2 + \mu_U^2} \frac{1}{x^{\alpha_{f_1}(0)}} + \\ &+ \frac{5\mu_U^2\beta_{f'_1qq}\beta_{f'_1NN}}{9\ 4\pi^3\Gamma(\alpha_{f'_1}(0))} \frac{Q^2}{Q^2 + \mu_U^2} \frac{1}{x^{\alpha_{f'_1}(0)}}, \\ g_1^{(3)}(x, Q^2) &= \frac{1\mu_U^2\beta_{a_1qq}\beta_{a_1NN}}{3\ 4\pi^3\Gamma(\alpha_{a_1}(0))} \frac{Q^2}{Q^2 + \mu_U^2} \frac{1}{x^{\alpha_{a_1}(0)}}. \end{aligned} \quad (16)$$

For the fit we use the available data on  $g_1(x, Q^2)$  [1] in the same kinematic region ( $Q^2 = 1 \div 3$  GeV<sup>2</sup> and  $x \lesssim 0.1$ ) which has been used above in fitting  $F_2(x, Q^2)$ . Unfortunately, the amount of data available from polarized lepton-nucleon scattering is much smaller than that in the unpolarized case. The number of fit parameters therefore had to be decreased in order to get a high fit quality. Thus we assume a degeneracy of the ‘normal’ isovector  $f'_1$  and isoscalar  $A_1$  trajectories, analogous to the well known case of the degeneracy of  $\omega$  and  $\rho$  trajectories. Moreover we take their coupling to quarks to be equal. Under these conditions the total contribution of the  $f'_1$  and  $A_1$  to the neutron structure function  $g_1^n$  exactly vanishes, as it should be in a valence  $SU(6)_W$  model for nucleon structure functions.

The resulting parameters are:

$$\begin{aligned} \alpha_{f_1}(0) &= 0.88 \pm 0.14, \\ \beta_{f_1qq}\beta_{f_1NN} &= -3.04 \pm 2.42 \text{ GeV}^{-2}, \\ \alpha_{f'_1}(0) &= \alpha_{A_1}(0) = 0.62 \pm 0.13, \\ \beta_{f'_1qq}\beta_{f'_1NN} &= \frac{3}{5}\beta_{A_1qq}\beta_{A_1NN} = 13.57 \pm 9.79 \text{ GeV}^{-2}; \\ \mu_U &= 1.45 \pm 0.59 \text{ GeV}, \end{aligned} \quad (17)$$

which yield a common  $\chi^2$  value of 31.8 for 53 data points (22 for  $g_1^p$ , 14 for  $g_1^n$  and 17 for  $g_1^d$ ). We found that using different values of  $\mu_U$  for the ‘anomalous’, isoscalar and isovector components does not provide a substantial improvement of the  $\chi^2$  value. Therefore we used the same  $\mu_U$  for the three channels.

As before, we take that the slopes of the  $f'_1$  and  $a_1$  exchanges to be the standard Reggeon value, i.e. 0.9 GeV<sup>-2</sup>, while for the  $f_1$  exchange we take the slope to

be zero, as established in Ref. [5]. We mention again that the effect of the slopes on the double-spin asymmetry is negligible.

The result of our fit to  $g_1(x, Q^2)$  in the Regge region  $x \lesssim 0.1$ , presented in Fig. 2- 4, leads to the conclusion that our model is in good agreement with the available data. This supports the expectation that it may describe not only the structure functions  $F_2$  and  $g_1$ , but – in the context of SCHC – also vector meson production at small values of  $-t$ .

#### IV. THE CROSS-SECTION OF VECTOR MESON ELECTROPRODUCTION

The cross-section of vector meson electroproduction reads (cf. Fig. 1b):

$$\frac{d\sigma}{d|t|} = \frac{|M(t)|^2}{64\pi W^2(\vec{q}_{cm})^2}, \quad (19)$$

where  $(\vec{q}_{cm})^2 = (W^4 + Q^4 + m_p^4 + 2W^2Q^2 - 2W^2m_p^2 + 2Q^2m_p^2)/4W^2$ ,  $W$  is the center-of-mass energy of the virtual-photon proton system and  $m_p$  is the proton mass.

It was found [7, 29, 30] that the main features of the photoproduction reaction can be reproduced within a simple non-relativistic model for the vector meson wave function, where the quark and the anti-quark form the meson only if they have equal momenta. Above  $Q^2 \approx 3$  GeV<sup>2</sup>, the quark’s off-shellness and Fermi motion inside the vector meson have to be taken into account [31]. At smaller  $Q^2$  these effects are not important and the non-relativistic model is applicable. In this framework, the Pomeron,  $f_2$  and  $A_2$  Reggeon exchange amplitudes read [7]

$$\begin{aligned} M_N &= 4C_R^N m_V \beta_{Rqq} \beta_{RNN} \sqrt{\frac{3m_V \Gamma_{e^+e^-}}{\alpha_{em}}} \bar{u}(p_2) \gamma_\alpha u(p_1) \times \\ &\times \frac{(g_{\mu\nu} q^\alpha - g_{\nu\alpha} p_V^\mu - g_{\mu\alpha} q^\nu) \varepsilon_\gamma^\mu \varepsilon_V^\nu}{q^2 + t - m_V^2} \times \\ &\times \frac{1 + \exp\{-i\pi\alpha(t)\}}{\sin\{\pi\alpha(t)\} \Gamma(\alpha_R(t))} \left(\frac{s}{Q^2}\right)^{\alpha_R(t)-1} F_R^V(t) \approx \\ &\approx \frac{8m_V \beta_{Rqq} \beta_{RNN} Q^2}{Q^2 - t + m_V^2} \sqrt{\frac{3m_V \Gamma_{e^+e^-}}{\alpha_{em}}} \times \\ &\times \frac{1 + \exp\{-i\pi\alpha(t)\}}{\sin\{\pi\alpha(t)\} \Gamma(\alpha_R(t))} \left(\frac{s}{Q^2}\right)^{\alpha_R(t)} F_R^V(t), \end{aligned} \quad (20)$$

where  $m_V$  is the mass of the vector meson,  $C_R^N = e_u - e_d$  for the Pomeron and  $f_2$  exchanges, while  $C_{a_2}^N = e_u + e_d$ , and  $\Gamma_{e^+e^-}$  is its leptonic width. The parameters of the exchanges have been fixed above:  $\beta_{Pqq} = \beta_{PNN}/3 = 1.6$  GeV<sup>-1</sup>,  $\beta_{f_2qq} = \beta_{f_2NN}/3 = 4.7$  GeV<sup>-1</sup>,  $\beta_{a_2qq} = \beta_{a_2NN} = 4.9$  GeV<sup>-1</sup>,  $\alpha_P(t) = 1.20 + 0.25 t$ ,  $\alpha_{f_2}(t) = 0.64 + 0.9 t$ ,  $\alpha_{a_2}(t) = 0.36 + 0.9 t$ . The vector form factor of the

Pomeron-NN vertex is [29]

$$F_P^V = \frac{4m_p^2 - 2.8t}{(4m_p^2 - t)(1 - t/0.71)^2}. \quad (21)$$

We assume that the Pomeron and  $f_2$  Reggeon vertices have the same form factors. An additional factor has to be included to take into account the non-locality of these vertices,

$$\frac{\mu_N^2}{\mu_N^2 + Q^2 - t}, \quad (22)$$

where  $\mu_N = 0.8$  GeV according to Eq. (4).

In a similar way one can obtain the unnatural-parity Reggeon contribution to the vector meson production amplitude [7].

$$\begin{aligned} M_U &= 4m_V C_R^U \beta_{Rqq} \beta_{RNN} \sqrt{\frac{3m_V \Gamma_{e^+e^-}}{\alpha_{em}}} \times \\ &\times \frac{\epsilon_{\mu\nu\alpha\beta} q^\beta \epsilon_V^\mu \bar{u}(p_2) \gamma_5 \gamma_\alpha u(p_1)}{q^2 + t - m_V^2} \frac{\mu_U^2}{Q^2 + \mu_U^2} F_R^A(t) \times \\ &\times \frac{1 - \exp\{-i\pi\alpha_R(t)\}}{\sin\{\pi\alpha_R(t)\} \Gamma(\alpha_R(t))} \left(\frac{s}{Q^2}\right)^{\alpha_R(t)-1} \approx \\ &\approx \frac{8C_R' \lambda_\gamma \lambda_p m_V \beta_{Rqq} \beta_{RNN} Q^2}{Q^2 - t + m_V^2} \sqrt{\frac{3m_V \Gamma_{e^+e^-}}{\alpha_{em}}} \times \\ &\times \frac{1 - \exp\{-i\pi\alpha_R(t)\}}{\sin\{\pi\alpha_R(t)\} \Gamma(\alpha_R(t))} \left(\frac{s}{Q^2}\right)^{\alpha_R(t)} \frac{\mu_U^2}{Q^2 + \mu_U^2} F_R^A(t), \end{aligned} \quad (23)$$

where  $\lambda_\gamma$  and  $\lambda_p$  are the helicities of the photon and the proton, respectively, and  $C_R^U = e_u - e_d$  for the ‘anomalous’  $f_1$  exchange and the ‘normal’  $f_1'$  Reggeon, while  $C_{a_1}^U = e_u + e_d$ . According to Eqs. (17)-(18), the central values of the parameters of the exchanges are:  $\alpha_{f_1}(t) = \alpha_{f_1}(0) = 0.88$ ,  $\beta_{f_1qq} \beta_{f_1NN} = -3.04$  GeV<sup>-2</sup>,  $\alpha_{f_1'}(t) = \alpha_{a_1}(t) = 0.622 + 0.9t$ ,  $\beta_{f_1'qq} \beta_{f_1'NN} = \frac{3}{5} \beta_{A_1qq} \beta_{A_1NN} = 13.57$  GeV<sup>-2</sup>,  $\mu_U = 1.45$  GeV.

The axial vector form factor in the Reggeon-nucleon vertex is given by [32]

$$F_R^A(t) = \frac{1}{(1 - t/1.17)^2}. \quad (24)$$

Only the transverse cross-section of  $\rho^0$  meson electroproduction is necessary to calculate double-spin asymmetries. As can be seen from Fig. 5, the model described above is in fair agreement with experimental data [33, 34].

It is, however, necessary to verify whether the assumption of  $s$ -channel helicity conservation is valid for the description of  $\rho^0$  electroproduction at HERMES. Otherwise, a large contribution from the spin-flip amplitude could exist which does not enter the matrix elements related to the structure functions and an important ingredient in the reaction mechanism could be lost. Experimentally [26] it was measured that the violation of SCHC is less than 10%.

## V. THE DOUBLE-SPIN ASYMMETRY IN $\rho^0$ MESON ELECTROPRODUCTION

Recently, HERMES has published data on a sizeable double-spin asymmetry in  $\rho^0$  meson electroproduction on the proton [35]. It is not expected that perturbative QCD calculations can explain this result, because for  $\rho^0$  production at HERMES energy there is no hard scale available. In general, pQCD calculations based on two gluon-exchange in the  $t$ -channel predict a very small asymmetry at  $t=0$  [36, 37]. The phenomenological Regge approach used here takes effectively into account non-perturbative effects of QCD which are important at HERMES energies.

The longitudinal double-spin asymmetry  $A_1^V$  for the interaction of transverse photons with a longitudinally polarized nucleon is defined as:

$$A_1^V(t) \equiv \frac{\sigma_T^{1/2} - \sigma_T^{3/2}}{\sigma_T^{1/2} + \sigma_T^{3/2}} = \frac{|M_T^{1/2}(t)|^2 - |M_T^{3/2}(t)|^2}{|M_T^{1/2}(t)|^2 + |M_T^{3/2}(t)|^2}. \quad (25)$$

Here  $M_T^{1/2}$  and  $M_T^{3/2}$  denote the transverse virtual photon scattering amplitudes where the superscript describes the projection of the total spin of the photon-nucleon system to the direction of the photon momentum. The amplitudes  $M_T^{1/2,3/2}$  contain spin-independent parts made up by exchanges with natural parity ( $M_N^{1/2,3/2}$ ) and spin-dependent parts made up by exchanges with unnatural parity ( $M_U^{1/2,3/2}$ ). Between them the following relations hold

$$M_N^{1/2}(t) = M_N^{3/2}(t), \quad M_U^{1/2}(t) = -M_U^{3/2}(t). \quad (26)$$

Then

$$\begin{aligned} A_1^V(t) &= 2 \frac{\text{Re}\{M_N^{1/2}(t)\} \text{Re}\{M_U^{1/2}(t)\}}{|M_N^{1/2}(t)|^2 + |M_U^{1/2}(t)|^2} + \\ &+ 2 \frac{\text{Im}\{M_N^{1/2}(t)\} \text{Im}\{M_U^{1/2}(t)\}}{|M_N^{1/2}(t)|^2 + |M_U^{1/2}(t)|^2}. \end{aligned} \quad (27)$$

At this point this asymmetry can be analyzed qualitatively. Both types of amplitudes contain real and imaginary parts. The sign of the imaginary part can be determined using the optical theorem, the sign of the real part follows from the Regge formula given in Eq. (1). The optical theorem reads

$$\sigma_{tot} = \frac{1}{s} \text{Im}\{M(s, 0)\}. \quad (28)$$

Since the total cross-section of photon-nucleon scattering is positive, the imaginary parts of the forward photon-nucleon scattering amplitude for Pomeron and  $f_2$  Reggeon exchanges are positive. It then follows from Eq. (1) that their real parts are negative. In the same way we deduce that the difference of imaginary parts of the photon-nucleon elastic scattering amplitude with anti-parallel and parallel spins  $\Delta M_U = M_U^{1/2} - M_U^{3/2} = 2M_U^{1/2}$

is positive if the contribution of the corresponding exchange to the structure function  $g_1(x, Q^2) \sim \sigma^{1/2} - \sigma^{3/2}$  is positive. The real part of  $\Delta M_U$  in this case is also positive. If the contribution to the spin structure function  $g_1(x, Q^2)$  is negative, the imaginary and real parts of the difference  $\Delta M_U$  are negative.

It is worthwhile to note that a direct estimate of the vector meson production asymmetry based on the relation  $A_1^V \approx 2A_1^{DIS}$  [38], even in the context of SCHC, does inherently not include the real part of the vector meson production amplitude as the DIS data on  $g_1$  and  $F_2$  are connected only to the imaginary part. For a full description, however, a way must be found to construct the real part which, in this paper, was chosen to be the Regge approach described above.

For the ‘anomalous’  $f_1$  exchange, the real part is much larger than the imaginary part and therefore this exchange should give a positive contribution to the asymmetry. For  $f_1'$  and  $a_1$  exchanges, real and imaginary parts of the amplitudes contribute with different signs to the asymmetry. For scattering on the proton, their real parts give a negative asymmetry, and the imaginary parts give a positive one. This is also the case for  $f_1'$  exchange when scattering on the neutron and on the deuteron. For  $a_1$  exchange in the case of scattering on the neutron, the real part of the amplitude leads to a positive double-spin asymmetry and the imaginary part leads to a negative one. Altogether, this discussion applies only to the region of small  $|t|$  where the corresponding amplitudes do not change sign ( $\alpha = 0$ ). Since the elastic cross-section originates mainly from the small  $|t|$  region, we expect this qualitative analysis to be valid.

The calculated predictions for double-spin asymmetries are shown in Figs. 6-13. Shaded areas were chosen to illustrate the range in the predictions obtained when different values for the ‘anomalous’  $f_1$  intercept are used. The upper limit of this range,  $0.74 - 0.93$  (cf. Eq. 17), is determined by the restriction that it is necessary to reproduce the transverse cross section shown in Fig. 5. Intercept values very close to unity are excluded, because otherwise the propagator in Eq. (1) would yield a too large contribution for  $\alpha_{f_1} \rightarrow 1$ .

From the figures it is evident that the contributions of the secondary  $f_1'$  and  $a_1$  Reggeons to the asymmetry are not small. At HERMES energies, they are of about the same size as the contribution of the ‘anomalous’  $f_1$  exchange which we considered previously [7] within another approach.

More information about the flavor composition of the asymmetry can be obtained when considering the case of the deuteron and the neutron. For the deuteron the isovector exchange contribution to  $A_1^V$  vanishes, and for the neutron it comes with the opposite sign and partly cancels the regular isoscalar part. By this reason the

‘anomalous’ part can be observed best when studying data on the neutron.

The dependencies of the double-spin asymmetry  $A_1^V$  on various kinematic variables are displayed in these figures for proton and deuteron. The Regge-based predictions were calculated for the HERMES kinematics,  $\langle W \rangle = 4.9$  GeV,  $\langle Q^2 \rangle = 1.7$  GeV<sup>2</sup>,  $\langle x \rangle = 0.07$ , and compared to measurements of  $\rho^0$  electroproduction at HERMES [35, 39, 40] on proton and deuteron. Although qualitative agreement can be seen only in the case of the proton, it is evident that experimental data with considerably improved precision are required.

## VI. CONCLUSIONS

In summary, the nucleon structure functions  $F_2(x, Q^2)$  and  $g_1(x, Q^2)$  were analyzed in the framework of a Regge approach. From the data on deep inelastic scattering on the proton, neutron and deuteron we derived the parameters of Reggeons with natural and unnatural parities in the region  $Q^2 = 1 \div 3$  GeV<sup>2</sup>. Using this parameterization and a non-relativistic model of  $\rho^0$  meson formation which provides a fair description of the cross-section, we calculated the double-spin asymmetry of  $\rho^0$  meson electroproduction at HERMES energies.

In this study we have used a unified approach to both DIS spin-dependent structure functions and vector meson electroproduction, in the context of  $s$ -channel helicity conservation. In this approach the obtained large value of the double-spin asymmetry in  $\rho^0$  meson production is correlated with the anomalous behavior of the flavor-singlet part of the structure function  $g_1(x, Q^2)$  at small  $x$ . In the case that future measurements will not confirm such a large asymmetry, for a Regge-type analysis it would have to be concluded that the ‘anomalous’  $f_1$  exchange is not a simple Regge pole but has a more complicated structure, e.g. a Regge cut.

## Acknowledgments

We are grateful to N.Bianchi, S.V.Goloskokov and O.V.Teryaev for useful discussions. This work was supported by the following grants RFBR-01-02-16431, INTAS-2000-366, EC-IHP-HPRN-CT-2000-00130, MCyT-BFM2001-0262, GV01-216, and by the Heisenberg-Landau program. A.V. thanks ICTP for the warm hospitality extended to him during his stay when a part of this work was completed and V.V. acknowledges the hospitality of Seoul National University during the last stages of this work.

---

[1] B. Adeva *et al.* [Spin Muon Collaboration], Phys. Rev. D **58**, 112001 (1998).

K. Abe *et al.* [E143 collaboration], Phys. Rev. D **58**,

- 112003 (1998).  
A. Airapetian *et al.* [HERMES Collaboration], Phys. Lett. B **442**, 484 (1998).  
P. L. Anthony *et al.* [E142 Collaboration], Phys. Rev. D **54**, 6620 (1996).  
K. Abe *et al.* [E154 Collaboration], Phys. Rev. Lett. **79**, 26 (1997).  
K. Ackerstaff *et al.* [HERMES Collaboration], Phys. Lett. B **404**, 383 (1997).
- [2] J. Bartels, B. I. Ermolaev and M. G. Ryskin, Z. Phys. C **72**, 627 (1996).  
[3] E. A. Kuraev, L. N. Lipatov and V. S. Fadin, Sov. Phys. JETP **45**, 199 (1977) [Zh. Eksp. Teor. Fiz. **72**, 377 (1977)].  
[4] V. S. Fadin and L. N. Lipatov, Phys. Lett. B **429**, 127 (1998).  
[5] N. I. Kochelev *et al.*, Phys. Rev. D **61**, 094008 (2000).  
[6] N. I. Kochelev *et al.*, Nucl. Phys. Proc. Suppl. **99A**, 24 (2001).  
[7] N. I. Kochelev, D. P. Min, V. Vento and A. V. Vinnikov, Phys. Rev. D **65**, 097504 (2002).  
[8] Y. Oh, N. I. Kochelev, D. P. Min, V. Vento and A. V. Vinnikov, Phys. Rev. D **62**, 017504 (2000).  
[9] P. D. Collins, "An Introduction To Regge Theory And High-Energy Physics," *Cambridge 1977*, 445p.  
[10] E. Levin, TAUP-2465-97, DESY-97-213, arXiv:hep-ph/9710546.  
[11] A. B. Kaidalov and Y. A. Simonov, Phys. Lett. B **477**, 163 (2000).  
[12] D. Kharzeev and E. Levin, Nucl. Phys. B **578**, 351 (2000).  
[13] E. V. Shuryak and I. Zahed, Phys. Rev. D **62**, 085014 (2000).  
[14] M. Guidal, J. M. Laget and M. Vanderhaeghen, Nucl. Phys. A **627**, 645 (1997).  
[15] S. I. Manaenkov, arXiv:hep-ph/9903405.  
[16] A. Donnachie and P. V. Landshoff, Phys. Lett. B **296**, 227 (1992).  
[17] D. E. Groom *et al.* [Particle Data Group Collaboration], Eur. Phys. J. C **15**, 1 (2000).  
[18] P. V. Landshoff and O. Nachtmann, Z. Phys. C **35**, 405 (1987).  
[19] A. Capella, A. Kaidalov, C. Merino and J. Tran Thanh Van, Phys. Lett. B **343**, 403 (1995).  
[20] C. Adloff *et al.* [H1 Collaboration], Phys. Lett. B **520**, 183 (2001).  
[21] J. Breitweg *et al.* [ZEUS Collaboration], Eur. Phys. J. C **7**, 609 (1999).  
[22] H. Abramowicz, E. M. Levin, A. Levy and U. Maor, Phys. Lett. B **269**, 465 (1991).  
A. Donnachie and P. V. Landshoff, Z. Phys. C **61**, 139 (1994).
- [23] M. R. Adams *et al.* [E665 Collaboration], Phys. Rev. D **54**, 3006 (1996).  
M. Arneodo *et al.* [New Muon Collaboration], Nucl. Phys. B **483**, 3 (1997).  
D. Allasia *et al.*, Z. Phys. C **28**, 321 (1985).  
S. Aid *et al.* [H1 Collaboration], Nucl. Phys. B **470**, 3 (1996).  
C. Adloff *et al.* [H1 Collaboration], Nucl. Phys. B **497**, 3 (1997).  
M. Derrick *et al.* [ZEUS Collaboration], Z. Phys. C **69**, 607 (1996).  
J. Breitweg *et al.* [ZEUS Collaboration], Eur. Phys. J. C **7**, 609 (1999).  
[24] J. Soffer and O. V. Teryaev, Phys. Rev. D **56**, 1549 (1997).  
S. D. Bass and M. M. Brisudova, Eur. Phys. J. A **4**, 251 (1999).  
[25] N. Bianchi and E. Thomas, Phys. Lett. B **450**, 439 (1999).  
[26] M. Tytgat, DESY-THESIS-2001-018.  
[27] L. Rosenberg, Phys. Rev. **129**, 2786 (1963).  
[28] M. Anselmino, A. Efremov and E. Leader, Phys. Rept. **261**, 1 (1995) [Erratum-ibid. **281**, 399 (1997)].  
[29] A. Donnachie and P. V. Landshoff, Phys. Lett. B **185**, 403 (1987).  
[30] J. M. Laget, Phys. Lett. B **489**, 313 (2000).  
[31] I. Royen and J. R. Cudell, Nucl. Phys. B **545**, 505 (1999).  
[32] A. Liesenfeld *et al.* [A1 Collaboration], Phys. Lett. B **468**, 20 (1999).  
[33] A. Airapetian *et al.* [HERMES Collaboration], Eur. Phys. J. C **17**, 389 (2000).  
[34] M. R. Adams *et al.* [E665 Collaboration], Z. Phys. C **74**, 237 (1997).  
[35] A. Airapetian *et al.* [HERMES Collaboration], Phys. Lett. B **513**, 301 (2001).  
[36] M. Vanttinen and L. Mankiewicz, Phys. Lett. B **440**, 157 (1998),  
M. Vanttinen and L. Mankiewicz, Phys. Lett. B **434**, 141 (1998).  
[37] S. V. Goloskokov, Eur. Phys. J. C **11**, 309 (1999).  
[38] H. Fraas, Nucl. Phys. B **113**, 532 (1976).  
N. N. Nikolaev, Nucl. Phys. Proc. Suppl. **79**, 343 (1999).  
[39] K. Lipka ( *for the HERMES Collaboration*), World Scientific, Proc. of PHOTON 2001, 186 (2002).  
[40] K. Lipka, talk at An International Conference on The Structure and Interactions of the Photon (PHOTON 2001), Ascona Switzerland September 2nd-7th 2001, <http://hep-proj-photon2001.web.cern.ch/hep-proj-photon2001/proc/proc.htm>

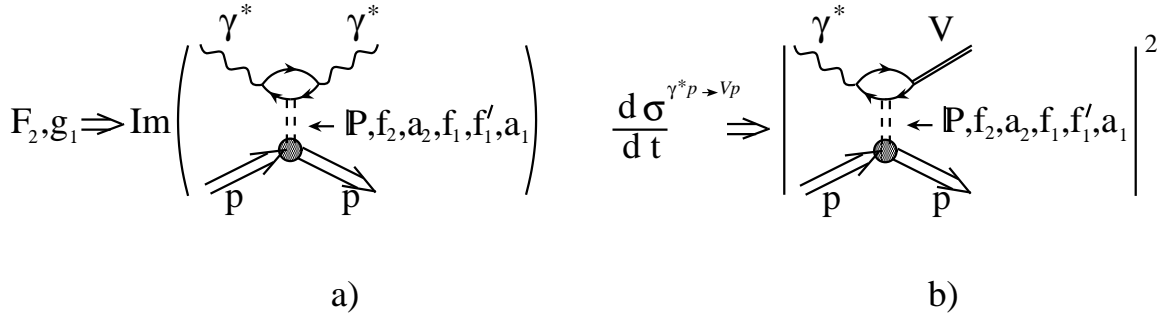


FIG. 1: S- channel helicity conservation implies that the same exchanges describe the structure functions ( $F_2$  and  $g_1$ ) of inclusive deep inelastic lepton scattering [panel a)] and of vector meson production processes at high energy [panel b)].

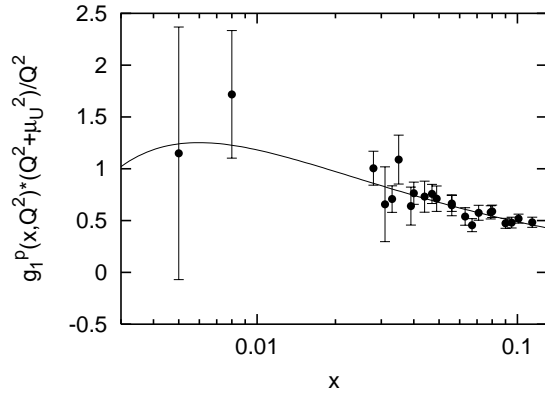


FIG. 2: The result of the fit of the proton structure function  $g_1(x, Q^2)$  in the Regge region ( $x < 0.1$ ) and at  $Q^2 = 1 - 3 \text{ GeV}^2$  in comparison with the data [1].

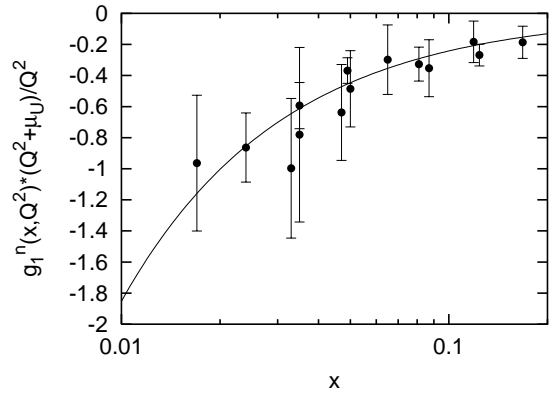


FIG. 3: The result of the fit of the neutron structure function  $g_1(x, Q^2)$  in the Regge region ( $x < 0.1$ ) and at  $Q^2 = 1 - 3 \text{ GeV}^2$  in comparison with the data [1].

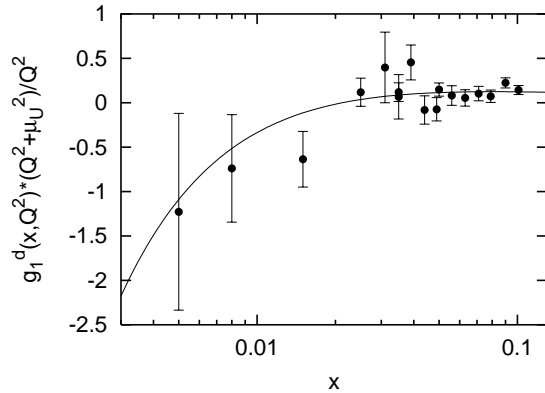


FIG. 4: The result of the fit of the deuteron structure function  $g_1(x, Q^2)$  in the Regge region ( $x < 0.1$ ) and at  $Q^2 = 1 - 3 \text{ GeV}^2$  in comparison with the data [1].

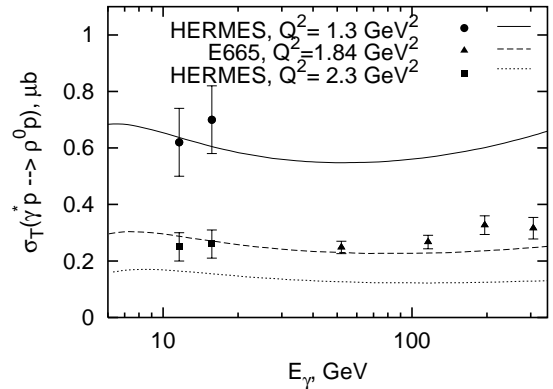


FIG. 5: The cross-section of  $\rho^0$  electroproduction by transverse photons is shown. The data points have been obtained from the published total and longitudinal cross-sections measured at HERMES [33] and E665 [34]. The solid, dashed and dotted lines represent the model calculations at the given  $Q^2$  values.



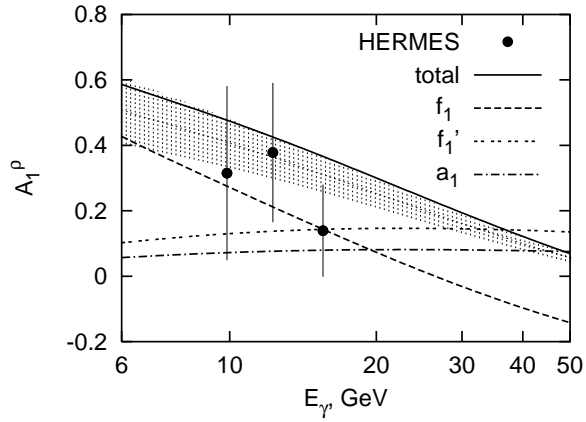


FIG. 6: The  $E_{\gamma^*}$ -dependence of the double-spin asymmetry  $A_1^p$  on the proton compared to data calculated from results of HERMES [35]. The shaded area corresponds to the interval of allowed values  $0.72 \div 0.93$  for the anomalous  $f_1$  intercept (see section V).

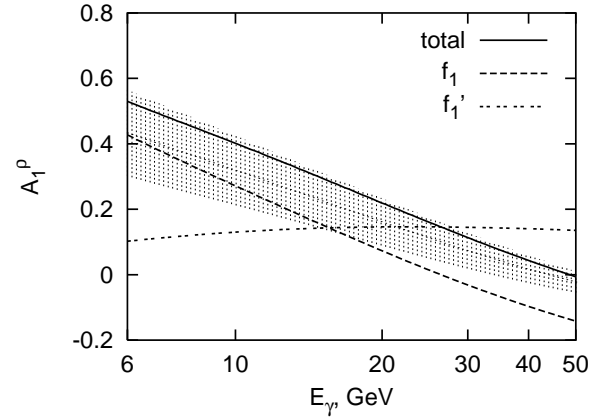


FIG. 7: The  $E_{\gamma^*}$ -dependence of the double-spin asymmetry  $A_1^p$  on the deuteron is shown. The notations are the same as in Fig. 6.

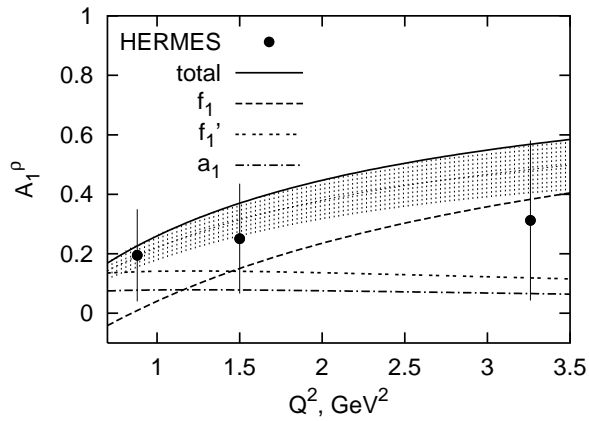


FIG. 8: The  $Q^2$ -dependence of the double-spin asymmetry  $A_1^p$  on the proton, compared to results of HERMES [35]. The notations are the same as in Fig. 6.

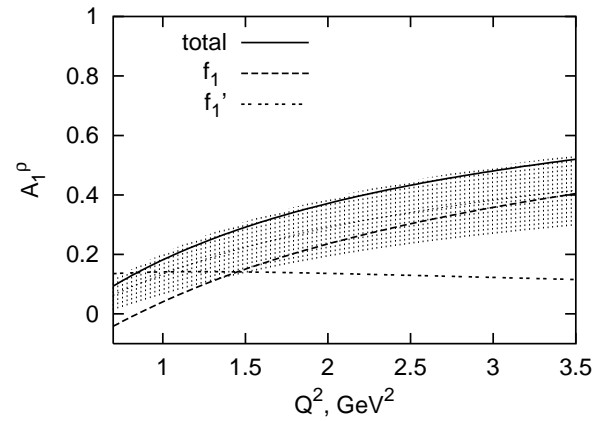


FIG. 9: The  $Q^2$ -dependence of the double-spin asymmetry  $A_1^p$  on the deuteron is shown. The notations are the same as in Fig. 6.

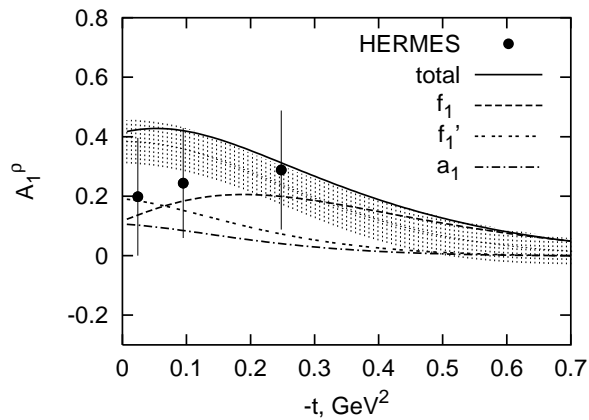


FIG. 10: The  $-t$ -dependence of the double-spin asymmetry  $A_1^p$  on the proton, compared to results of HERMES [35]. The notations are the same as in Fig. 6.

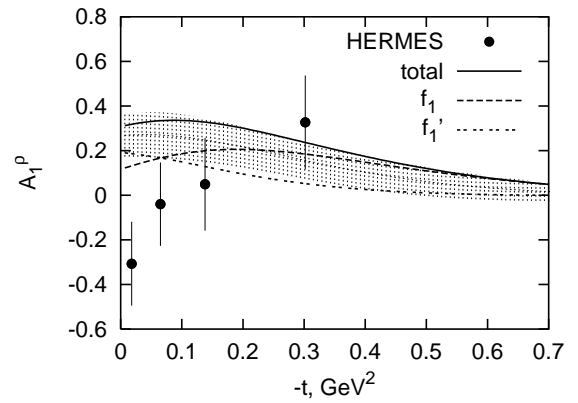


FIG. 11: The  $-t$ -dependence of the double-spin asymmetry  $A_1^p$  on the deuteron, compared to preliminary results of HERMES [40]. The notations are the same as in Fig. 6.

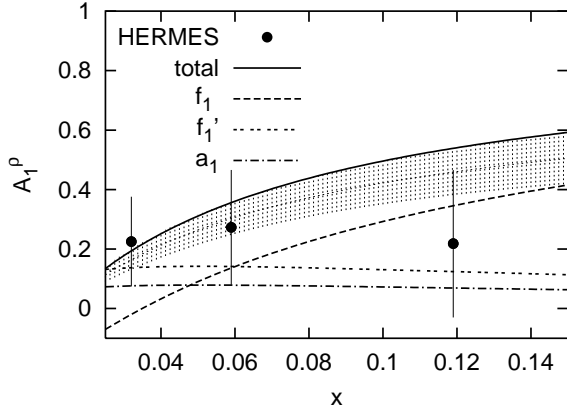


FIG. 12: The  $x$ -dependence of the double-spin asymmetry  $A_1^p$  on the proton, compared to results of HERMES [35]. The notations are the same as in Fig. 6.

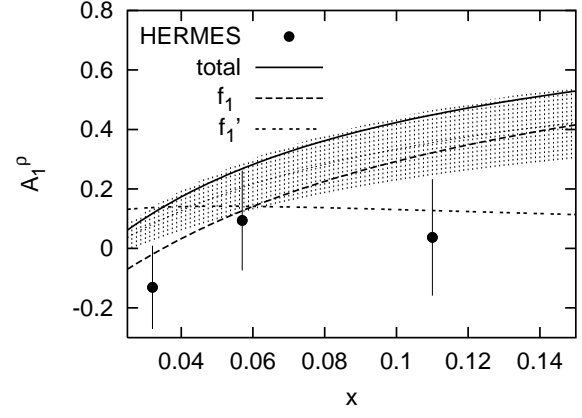


FIG. 13: The  $x$ -dependence of the double-spin asymmetry  $A_1^p$  on the deuteron, compared to preliminary results of HERMES [39]. The notations are the same as in Fig. 6.

# DIS structure functions and the double-spin asymmetry in $\rho^0$ electroproduction within a Regge approach

N.I. Kochelev\*

*Bogoliubov Laboratory of Theoretical Physics, JINR, Dubna, Moscow region, 141980 Russia<sup>†</sup>*

K. Lipka<sup>‡</sup> and W.-D. Nowak<sup>§</sup>  
*DESY Zeuthen, 15738 Zeuthen, Germany*

V. Vento<sup>¶</sup>  
*Departament de Física Teòrica and Institut de Física Corpuscular,  
Universitat de València-CSIC E-46100, Burjassot (Valencia), Spain*

A.V. Vinnikov\*\*

*Bogoliubov Laboratory of Theoretical Physics, JINR, Dubna, Moscow region, 141980 Russia<sup>††</sup>*

(Dated: December 11, 2002)

The proton, neutron and deuteron structure functions  $F_2(x, Q^2)$  and  $g_1(x, Q^2)$ , measured at intermediate  $Q^2$ , are analyzed within a Regge approach. This analysis serves to fix the parameters of this scheme which are then used to calculate, in a unified Regge approach, the properties of  $\rho^0$  meson electroproduction on the proton and the deuteron. In this way, the double-spin asymmetry observed at HERMES in  $\rho^0$  electroproduction on the proton, can be related to the anomalous behavior of the flavor-singlet part of the spin-dependent structure function  $g_1(x, Q^2)$  at small  $x$ .

PACS numbers: 12.40.Nn, 13.60.Le, 13.75.Cs, 13.88.+e

## I. INTRODUCTION

Understanding the spin structure of the nucleon is today one of the main problems in hadron physics. Polarized beams have allowed significant progress in the measurement of the nucleon spin-dependent structure functions in the Deep Inelastic Scattering (DIS) regime. A result of some of these measurements [1] is that, at small values of Bjørken  $x$ , the neutron spin-dependent structure function  $g_1^n(x, Q^2)$ , which according to the  $SU(6)_W$  model is dominated by the flavor singlet quark sea part, exhibits an anomalous behavior. More precisely, at  $x \rightarrow 0$ ,  $g_1^n(x, Q^2) \sim 1/x$ , while the expected behavior should be  $1/x^{\alpha_{a_1}}$ , where  $a_1$  is a conventional Regge trajectory with appropriate quantum numbers and intercept  $\alpha_{a_1} = -0.5 \div 0.5$ . Experimental data are thus well described in terms of a leading trajectory with an intercept close to 1, a value reminiscent of the Pomeron. In fact, this type of behavior at small  $x$  was predicted by leading order perturbative QCD calculations [2]. However, since next-to-leading order corrections to the perturbative BFKL Pomeron [3] are large [4], it is not clear to

which extent the perturbative description is valid.

In Ref. [5], the observed anomalous behavior of  $g_1^n(x, Q^2)$ , was assumed to signal the existence of a flavor-singlet exchange with large intercept and negative signature, which was then used to explain the experimental data on diffractive hadronic reactions: vector meson photoproduction at  $\sqrt{s} \approx 100$  GeV,  $|t|=1 \div 10$  GeV<sup>2</sup> and proton-proton elastic scattering at  $\sqrt{s}=20 \div 60$  GeV,  $|t|=2 \div 10$  GeV<sup>2</sup> [5, 6]. This exchange gives sizeable contributions to the differential cross-sections at large energy due to the large value of its intercept. We called it  $f_1$  since its quantum numbers coincide with those of the axial vector  $f_1(1285)$  meson ( $P=C=+1$ , negative signature). The mechanism leading to this exchange in QCD is not known. The relation of the Pomeron with the scale anomaly, led us to conjecture a relation between the  $f_1$  and the gluonic axial anomaly, since the  $f_1$  strongly mixes with gluonic degrees of freedom [5].

In order to investigate this unnatural-parity exchange the best observables are spin-dependent cross-sections. For example, we already have shown that the  $f_1$  exchange leads to large double-spin asymmetries in different diffractive reactions [5, 7, 8].

For  $s$ -channel helicity conserving (SCHC) reactions it seems reasonable, in the context of the VMD model, to establish a relation between the matrix elements describing the structure functions and vector meson electroproduction at low  $-t$ , as indicated in Fig. 1. This relation arises naturally in the context of the Regge approach [9], where the imaginary part of the forward Compton scattering amplitude, relevant to describe DIS structure functions, and the total amplitude for vector meson production at  $-t \rightarrow 0$  are connected.

---

\*Electronic address: kochelev@thsun1.jinr.ru

<sup>†</sup>Also at Institute of Physics and Technology, Almaty, 480082, Kazakhstan

<sup>‡</sup>Electronic address: Katerina.Lipka@desy.de

<sup>§</sup>Electronic address: Wolf.Dieter.Nowak@desy.de

<sup>¶</sup>Electronic address: vicente.vento@uv.es

\*\*Electronic address: vinnikov@thsun1.jinr.ru

<sup>††</sup>Also at School of Physics, Seoul National University, Seoul 151-747, Korea

The Regge model is a well known approach to describe diffractive reactions with small momentum transfer and high energy, a kinematic region where non-perturbative QCD effects are important. For this reason the investigation of diffraction and structure functions at low  $x$  are important items included into the experimental programs of the current and future accelerators: HERA, TEVATRON, RHIC, LHC, etc. These studies are expected to considerably enlarge the insight into the nature of strong interactions between quarks at large distances [10]. Several scenarios for the direct relation between the complex structure of the QCD vacuum and Regge behavior have been suggested [11–13].

The effective propagator for the spin-nonflip amplitude for scattering of two particles with momenta  $p_1$  and  $p_2$  has the following form in Regge theory:

$$D_R(s, t) = -\frac{1}{\sin(\pi\alpha_R(t))\Gamma(\alpha_R(t))} \left(\frac{s}{s_0}\right)^{\alpha_R(t)-1} \times \\ \times \left[1 + \sigma_R \cos(\pi\alpha_R(t)) - i \cdot \sigma_R \sin(\pi\alpha_R(t))\right], \quad (1)$$

where  $s = (p_1 + p_2)^2$ ,  $t = (p_1 - p_2)^2$ ,  $s_0$  is  $\max(p_1^2, p_2^2, p_1'^2, p_2'^2)$ ,  $\alpha_R(t)$  describes the Regge trajectory of the particles exchanged in the  $t$  channel and  $\sigma_R$  their signature, related to the spin  $J$  by  $\sigma = (-1)^J$ . The  $\Gamma$  function in the denominator provides the correct analytic behavior of the amplitude [14]. In many cases, a simpler formula can be used [15], but we prefer the original form in order to keep a precise relation between the real and the imaginary parts of the amplitude. This relation will be used below to establish a connection between the properties of the DIS structure functions and those of vector meson electroproduction off the nucleon as suggested above.

Reggeons, with signature and space parities of the same sign,  $\sigma = P$  (natural parity), have an amplitude which does not depend on the helicities of the colliding particles. Their exchange gives the dominant contributions to the spin-independent nucleon structure functions and to the total cross-sections. Exchanges with unnatural parity,  $\sigma = -P$ , have an amplitude which is proportional to the product of the particle helicities. Thus, only Reggeons with unnatural parities can contribute to the spin-dependent structure function  $g_1(x, Q^2)$ . Furthermore, a longitudinal double-spin asymmetry in two-particle scattering only arises when an unnatural-parity-exchange contribution to the scattering amplitude exists.

The main goal of this paper is an analysis of the deep-inelastic structure functions  $F_2(x, Q^2)$  and  $g_1(x, Q^2)$  in the framework of the Regge model; the extracted Reggeon parameters will be used to calculate the elastic cross-section, and finally the double-spin asymmetry, of  $\rho^0$  electroproduction for intermediate values of  $Q^2$ .

The Regge scheme will be defined by the exchange of trajectories with very large intercepts (Pomeron and the ‘anomalous’ component of  $f_1$ ) and of secondary Regge trajectories, namely  $f_2$ ,  $a_2$ , the ‘normal’ component of

$f_1$  (which will be called  $f_1'$ ) and  $a_1$ . Especially the contributions of secondary Reggeons are considered to be of importance at HERMES energies,  $\sqrt{s} = 7$  GeV.

## II. THE STRUCTURE FUNCTION $F_2(x, Q^2)$ IN A REGGE APPROACH AT INTERMEDIATE VALUES OF $Q^2$

The parameters of the natural-parity Reggeons in soft interactions ( $Q^2 < 1$  GeV<sup>2</sup>) are quite well known. They can be obtained from fits to the total hadronic cross-sections [16]. In particular, the parameters of the Pomeron,  $f_2$  and  $a_2$  Reggeon trajectories which are relevant for our calculation, are given by the Particle Data Group [17]:

$$\alpha_P(t) = 1.093 + 0.25 t, \beta_{Pqq} = \beta_{PNN}/3 = 1.6 \text{ GeV}^{-1}, \\ \alpha_{f_2}(t) = 0.358 + 0.9 t, \beta_{f_2qq} = \beta_{f_2NN}/3 = 4.7 \text{ GeV}^{-1}, \\ \alpha_{a_2}(t) = 0.545 + 0.9 t, \beta_{a_2qq} = \beta_{a_2NN} = 4.9 \text{ GeV}^{-1}, \quad (2)$$

where  $\beta_{RNN}$  and  $\beta_{Rqq}$  are the coupling constants for the Reggeon-nucleon and Reggeon-quark couplings, respectively. The effective Lorentz structure of the coupling of these Reggeons to nucleons and quarks is assumed to be  $\gamma_\mu$  [18]. The values of the slopes of the trajectories, which cannot be obtained from a fit to the total hadronic cross-sections, are taken from Ref. [9]. The relation between the couplings to quarks and nucleons is obtained from the naive constituent quark model. A clear separation of the secondary Reggeons and the Pomeron is possible because the energy dependencies of their amplitudes described by the intercepts  $\alpha(0)$ ,  $\sigma_R^{tot} \sim s^{\alpha_R(0)-1}$  are very different. Specifically, the Pomeron contribution to the total hadronic cross-section rises as  $s^{0.093}$ , while, for example, the  $f_2$  contribution falls as  $s^{-0.642}$ .

For large virtualities of the scattering particles, the effective intercepts of the Pomeron and the Reggeons change [19]. In particular, it was measured by the H1 and ZEUS Collaborations at HERA [20, 21] that the effective Pomeron intercept, extracted from the analysis of the  $F_2(x, Q^2)$  structure function, ranges from about 1.1 at  $Q^2 \approx 0$  to about 1.4 at  $Q^2 > 10^2$  GeV<sup>2</sup>. Therefore, to make predictions for HERMES ( $< Q^2 > = 1.7$  GeV<sup>2</sup>), knowledge of the Pomeron and Reggeons intercepts at  $Q^2$  values of a few GeV<sup>2</sup> is required.

The Regge formulae [22] for the proton and deuteron structure functions used are

$$F_2^p(x, Q^2) = \frac{Q^2}{Q^2 + \mu_N^2} \times \\ \times \left( \frac{A_P}{x^{\alpha_P(0)-1}} + \frac{A_{f_2}}{x^{\alpha_{f_2}(0)-1}} + \frac{A_{a_2}}{x^{\alpha_{a_2}(0)-1}} \right), \\ F_2^d(x, Q^2) = \frac{Q^2}{Q^2 + \mu_N^2} \left( \frac{A_P}{x^{\alpha_P(0)-1}} + \frac{A_{f_2}}{x^{\alpha_{f_2}(0)-1}} \right). \quad (3)$$

The various structure functions appearing in these equations represent the  $SU(3)_f$  flavor singlet (the Pomeron),

the  $SU(2)_f$  isoscalar ( $f_2$ ) and the isovector ( $a_2$ ) exchanges. The parameter  $\mu_N$  effectively accounts for the scaling violation at small  $Q^2$  for the natural parity exchanges. Using Eq. (3) we made a fit (not shown) to the recent  $F_2$  data [23] at  $Q^2 = 1 \div 3 \text{ GeV}^2$  and  $x \lesssim 0.1$  (Regge region). The extracted parameters of Pomeron,  $f_2$  and  $a_2$  Reggeons are

$$\begin{aligned} A_P &= 0.15 \pm 0.02, & \alpha_P(0) &= 1.20 \pm 0.01; \\ A_{f_2} &= 0.46 \pm 0.05, & \alpha_{f_2}(0) &= 0.61 \pm 0.07; \\ A_{a_2} &= 0.12 \pm 0.11, & \alpha_{a_2}(0) &= 0.36 \pm 0.28; \\ \mu_N &= 0.80 \pm 0.02 \text{ GeV}. \end{aligned} \quad (4)$$

This fit provides a value of  $\chi^2 = 191.2$  for 164 data points ( $\chi^2/\text{ndof}=1.17$ ). It is evident that already in the semi-hard region ( $Q^2$ -values of a few  $\text{GeV}^2$ ) modified Regge intercepts have to be used. The slopes can be assumed to remain unchanged as they seem to vary quite slowly in this  $Q^2$  region [26]. Moreover, they have no strong effect on the double-spin asymmetry.

### III. THE SPIN-DEPENDENT STRUCTURE FUNCTION $g_1(x, Q^2)$ IN A REGGE APPROACH.

Parameters for unnatural-parity Reggeons have been extracted earlier using Regge-type *phenomenological fits* to the spin-dependent structure function  $g_1(x, Q^2)$  [24, 25]. In our approach not only effective intercepts of Regge exchanges are determined, but also their couplings with nucleons and quarks. These couplings are a necessary input to the calculation of the double-spin asymmetry in vector meson electroproduction (see below). We use the relation between  $g_1(x, Q^2)$  and the imaginary part of the spin-dependent forward Compton scattering amplitude. By *direct calculation* (Fig. 1a) the contribution of the unnatural-parity-Reggeon exchanges to this amplitude is obtained as:

$$\begin{aligned} T^{\mu\nu}(q, p, S) &= \beta_{Rqq} \beta_{RNN} C_R \bar{u}(p, S) \gamma_\alpha \gamma_5 u(p, S) \times \\ &\times R^{\mu\nu\alpha} \frac{1 - \exp\{-i\pi\alpha_R(0)\}}{\sin\{\pi\alpha_R(0)\}} \left(\frac{2p \cdot q}{s_0}\right)^{\alpha_R(0)-1}, \end{aligned} \quad (5)$$

where we assume that all exchanges  $f_1$ ,  $f'_1$  and  $a_1$  have a  $\gamma_\alpha \gamma_5$  Lorenz structure for both the quark and the nucleon vertices. The nucleon spin is denoted by  $S$ , and  $s_0 \approx Q^2$  is the characteristic scale in the process.

The factor  $C_R$  is given by  $e_u^2 + e_d^2 + e_s^2$  for the  $SU(3)_f$  singlet ‘anomalous’ exchange ( $f_1$ ), by  $e_u^2 + e_d^2$  for the  $SU(2)_f$  singlet ‘normal’ exchange ( $f'_1$ ) and by  $e_u^2 - e_d^2$  for the  $SU(2)_f$  triplet  $a_1$ ;  $R^{\mu\nu\alpha}$  is given by Ref. [27]

$$\begin{aligned} R^{\mu\nu\alpha} &= -2 \int \frac{d^4 k}{(2\pi)^4} \frac{1}{(k^2 - m_q^2)((k - q)^2 - m_q^2)^2} \times \\ &Tr[(m_q + \hat{k} + \hat{q})\gamma^\nu (m_q + \hat{k})\gamma^\nu (m_q + \hat{k} + \hat{q})\gamma^\alpha \gamma_5], \end{aligned} \quad (6)$$

where  $m_q$  is the mass of the quark in the quark loop in Fig. 1.

Using the relation  $\bar{u}(p, S)\gamma_\alpha\gamma_5 u(p, S) = 2mS_\alpha$ , and the formula

$$R^{\mu\nu\alpha} = \frac{1}{2\pi^2} q_\tau \epsilon^{\tau\mu\nu\alpha}, \quad (7)$$

for  $-q^2 \gg m_q^2$  [28] we have

$$\begin{aligned} T^{\mu\nu}(q, p, S) &= \frac{m}{\pi^2} C_R \beta_{Rqq} \beta_{RNN} S_\alpha q_\tau \epsilon^{\tau\mu\nu\alpha} \times \\ &\times \frac{1 - \exp\{-i\pi\alpha_R(0)\}}{\sin\{\pi\alpha_R(0)\}} \Gamma(\alpha_R(0)) \left(\frac{2p \cdot q}{Q^2}\right)^{\alpha_R(0)-1}. \end{aligned} \quad (8)$$

This expression is compared to the general form

$$\begin{aligned} T_{(spin)}^{\mu\nu} &= i\epsilon^{\mu\nu\alpha\beta} q_\alpha S_\beta \frac{m}{pq} T_3 + \\ &+ i\epsilon^{\mu\nu\alpha\beta} q_\alpha (S_\beta(p \cdot q) - p_\beta(S \cdot q)) \frac{m}{(p \cdot q)^2} T_4, \end{aligned} \quad (9)$$

where the DIS structure functions  $g_1$  and  $g_2$  are related to the amplitudes  $T_3, T_4$  by

$$g_1(q, \nu) = -\frac{Im(T_3)}{2\pi}, \quad g_2(q, \nu) = -\frac{Im(T_4)}{2\pi}, \quad (10)$$

and where  $\nu = p \cdot q$ .

By assuming that the structure function  $g_2$  is small, we obtain

$$g_1(q, \nu) = \frac{\nu C_R \beta_{Rqq} \beta_{RNN}}{2\pi^3 \Gamma(\alpha_R(0))} \left(\frac{\nu}{Q^2}\right)^{\alpha_R(0)-1} \quad (11)$$

Using  $x = Q^2/2\nu$  we have

$$g_1(x, Q^2) = \frac{C_R \beta_{Rqq} \beta_{RNN}}{4\pi^3 \Gamma(\alpha_R(0))} \frac{Q^2}{x^{\alpha_R(0)}}. \quad (12)$$

This form does not yet provide the correct scaling behavior for the structure function at  $Q^2 \rightarrow \infty$  since the non-locality of the Reggeon-quark vertex in Fig. 1a was not taken into account. Phenomenologically, this can be accomplished by introducing a form factor (as has been done in the Pomeron case [29]):

$$F(Q^2) = \frac{\mu_U^2}{Q^2 + \mu_U^2}, \quad (13)$$

where  $\mu_U$  is the effective parameter describing the scaling violation at low  $Q^2$  for the unnatural-parity Reggeons. Then the contribution of a Reggeon to the  $g_1(x, Q^2)$  structure function reads

$$g_1(x, Q^2) = \frac{\mu_U^2 C_R \beta_{Rqq} \beta_{RNN}}{4\pi^3 \Gamma(\alpha_R(0))} \frac{Q^2}{Q^2 + \mu_U^2} \frac{1}{x^{\alpha_R(0)}} \quad (14)$$

which provides the correct scaling behavior of the structure function at large  $Q^2$ .

The parameters of the Reggeons with unnatural parity can be found from a fit to the available data on polarized DIS. Since data exist for proton, neutron and deuteron

targets, this allows the separation of the isoscalar and isovector parts of the respective structure functions

$$\begin{aligned} g_1^p(x, Q^2) &= g_1^{(1)}(x, Q^2) + g_1^{(3)}(x, Q^2), \\ g_1^n(x, Q^2) &= g_1^{(1)}(x, Q^2) - g_1^{(3)}(x, Q^2), \\ g_1^d(x, Q^2) &= g_1^{(1)}(x, Q^2), \end{aligned} \quad (15)$$

where  $g_1^{(1)}(x, Q^2)$  and  $g_1^{(3)}(x, Q^2)$  are the isoscalar and isovector components, respectively.

It was pointed out [24] that the isoscalar part contains two components: ‘normal’ and ‘anomalous’. The ‘normal’ component has an intercept of  $\alpha(0) \approx 0.5$  while the ‘anomalous’ has a large intercept,  $\alpha(0)$  close to 1. Using Eq. (14), the structure functions in Eq. (15) can be written

$$\begin{aligned} g_1^{(1)}(x, Q^2) &= \frac{2}{3} \frac{\mu_U^2 \beta_{f_1 qq} \beta_{f_1 NN}}{4\pi^3 \Gamma(\alpha_{f_1}(0))} \frac{Q^2}{Q^2 + \mu_U^2} \frac{1}{x^{\alpha_{f_1}(0)}} + \\ &+ \frac{5}{9} \frac{\mu_U^2 \beta_{f_1' qq} \beta_{f_1' NN}}{4\pi^3 \Gamma(\alpha_{f_1'}(0))} \frac{Q^2}{Q^2 + \mu_U^2} \frac{1}{x^{\alpha_{f_1'}(0)}}, \\ g_1^{(3)}(x, Q^2) &= \frac{1}{3} \frac{\mu_U^2 \beta_{a_1 qq} \beta_{a_1 NN}}{4\pi^3 \Gamma(\alpha_{a_1}(0))} \frac{Q^2}{Q^2 + \mu_U^2} \frac{1}{x^{\alpha_{a_1}(0)}}. \end{aligned} \quad (16)$$

For the fit we use the available data on  $g_1(x, Q^2)$  [1] in the same kinematic region ( $Q^2 = 1 \div 3$  GeV<sup>2</sup> and  $x \lesssim 0.1$ ) which has been used above in fitting  $F_2(x, Q^2)$ . Unfortunately, the amount of data available from polarized lepton-nucleon scattering is much smaller than that in the unpolarized case. The number of fit parameters therefore had to be decreased in order to get a high fit quality. Thus we assume a degeneracy of the ‘normal’ isovector  $f_1'$  and isoscalar  $A_1$  trajectories, analogous to the well known case of the degeneracy of  $\omega$  and  $\rho$  trajectories. Moreover we take their coupling to quarks to be equal. Under these conditions the total contribution of the  $f_1'$  and  $A_1$  to the neutron structure function  $g_1^n$  exactly vanishes, as it should be in a valence  $SU(6)_W$  model for nucleon structure functions.

The resulting parameters are:

$$\begin{aligned} \alpha_{f_1}(0) &= 0.88 \pm 0.14, \\ \beta_{f_1 qq} \beta_{f_1 NN} &= -3.04 \pm 2.42 \text{ GeV}^{-2}, \\ \alpha_{f_1'}(0) &= \alpha_{A_1}(0) = 0.62 \pm 0.13, \\ \beta_{f_1' qq} \beta_{f_1' NN} &= \frac{3}{5} \beta_{A_1 qq} \beta_{A_1 NN} = 13.57 \pm 9.79 \text{ GeV}^{-2}; \\ \mu_U &= 1.45 \pm 0.59 \text{ GeV}, \end{aligned} \quad (18)$$

which yield a common  $\chi^2$  value of 31.8 for 53 data points (22 for  $g_1^p$ , 14 for  $g_1^n$  and 17 for  $g_1^d$ ). We found that using different values of  $\mu_U$  for the ‘anomalous’, isoscalar and isovector components does not provide a substantial improvement of the  $\chi^2$  value. Therefore we used the same  $\mu_U$  for the three channels.

As before, we take that the slopes of the  $f_1'$  and  $a_1$  exchanges to be the standard Reggeon value, i.e. 0.9 GeV<sup>-2</sup>, while for the  $f_1$  exchange we take the slope to

be zero, as established in Ref. [5]. We mention again that the effect of the slopes on the double-spin asymmetry is negligible.

The result of our fit to  $g_1(x, Q^2)$  in the Regge region  $x \lesssim 0.1$ , presented in Fig. 2- 4, leads to the conclusion that our model is in good agreement with the available data. This supports the expectation that it may describe not only the structure functions  $F_2$  and  $g_1$ , but – in the context of SCHC – also vector meson production at small values of  $-t$ .

#### IV. THE CROSS-SECTION OF VECTOR MESON ELECTROPRODUCTION

The cross-section of vector meson electroproduction reads (cf. Fig. 1b):

$$\frac{d\sigma}{d|t|} = \frac{|M(t)|^2}{64\pi W^2 (\vec{q}_{cm})^2}, \quad (19)$$

where  $(\vec{q}_{cm})^2 = (W^4 + Q^4 + m_p^4 + 2W^2Q^2 - 2W^2m_p^2 + 2Q^2m_p^2)/4W^2$ ,  $W$  is the center-of-mass energy of the virtual-photon proton system and  $m_p$  is the proton mass.

It was found [7, 29, 30] that the main features of the photoproduction reaction can be reproduced within a simple non-relativistic model for the vector meson wave function, where the quark and the anti-quark form the meson only if they have equal momenta. Above  $Q^2 \approx 3$  GeV<sup>2</sup>, the quark’s off-shellness and Fermi motion inside the vector meson have to be taken into account [31]. At smaller  $Q^2$  these effects are not important and the non-relativistic model is applicable. In this framework, the Pomeron,  $f_2$  and  $A_2$  Reggeon exchange amplitudes read [7]

$$\begin{aligned} M_N &= 4C_R^N m_V \beta_{Rqq} \beta_{RNN} \sqrt{\frac{3m_V \Gamma_{e^+e^-}}{\alpha_{em}}} \bar{u}(p_2) \gamma_\alpha u(p_1) \times \\ &\times \frac{(g_{\mu\nu} q^\alpha - g_{\nu\alpha} P_V^\mu - g_{\mu\alpha} q^\nu) \varepsilon_\gamma^\mu \varepsilon_V^\nu}{q^2 + t - m_V^2} \times \\ &\times \frac{1 + \exp\{-i\pi\alpha(t)\}}{\sin\{\pi\alpha(t)\} \Gamma(\alpha_R(t))} \left(\frac{s}{Q^2}\right)^{\alpha_R(t)-1} F_R^V(t) \approx \\ &\approx \frac{8m_V \beta_{Rqq} \beta_{RNN} Q^2}{Q^2 - t + m_V^2} \sqrt{\frac{3m_V \Gamma_{e^+e^-}}{\alpha_{em}}} \times \\ &\times \frac{1 + \exp\{-i\pi\alpha(t)\}}{\sin\{\pi\alpha(t)\} \Gamma(\alpha_R(t))} \left(\frac{s}{Q^2}\right)^{\alpha_R(t)} F_R^V(t), \end{aligned} \quad (20)$$

where  $m_V$  is the mass of the vector meson,  $C_R^N = e_u - e_d$  for the Pomeron and  $f_2$  exchanges, while  $C_{a_2}^N = e_u + e_d$ , and  $\Gamma_{e^+e^-}$  is its leptonic width. The parameters of the exchanges have been fixed above:  $\beta_{Pqq} = \beta_{PNN}/3 = 1.6$  GeV<sup>-1</sup>,  $\beta_{f_2 qq} = \beta_{f_2 NN}/3 = 4.7$  GeV<sup>-1</sup>,  $\beta_{a_2 qq} = \beta_{a_2 NN} = 4.9$  GeV<sup>-1</sup>,  $\alpha_P(t) = 1.20 + 0.25 t$ ,  $\alpha_{f_2}(t) = 0.64 + 0.9 t$ ,  $\alpha_{a_2}(t) = 0.36 + 0.9 t$ . The vector form factor of the

$$F_P^V = \frac{4m_p^2 - 2.8t}{(4m_p^2 - t)(1 - t/0.71)^2}. \quad (21)$$

We assume that the Pomeron and  $f_2$  Reggeon vertices have the same form factors. An additional factor has to be included to take into account the non-locality of these vertices,

$$\frac{\mu_N^2}{\mu_N^2 + Q^2 - t}, \quad (22)$$

where  $\mu_N = 0.8$  GeV according to Eq. (4).

In a similar way one can obtain the unnatural-parity Reggeon contribution to the vector meson production amplitude [7].

$$\begin{aligned} M_U &= 4m_V C_R^U \beta_{Rqq} \beta_{RNN} \sqrt{\frac{3m_V \Gamma_{e^+e^-}}{\alpha_{em}}} \times \\ &\times \frac{\epsilon_{\mu\nu\alpha\beta} q^\beta \epsilon_\gamma^\mu \epsilon_V^\nu \bar{u}(p_2) \gamma_5 \gamma_\alpha u(p_1)}{q^2 + t - m_V^2} \frac{\mu_U^2}{Q^2 + \mu_U^2} F_R^A(t) \times \\ &\times \frac{1 - \exp\{-i\pi\alpha_R(t)\}}{\sin\{\pi\alpha_R(t)\} \Gamma(\alpha_R(t))} \left(\frac{s}{Q^2}\right)^{\alpha_R(t)-1} \approx \\ &\approx \frac{8C'_R \lambda_\gamma \lambda_p m_V \beta_{Rqq} \beta_{RNN} Q^2}{Q^2 - t + m_V^2} \sqrt{\frac{3m_V \Gamma_{e^+e^-}}{\alpha_{em}}} \times \quad (23) \\ &\times \frac{1 - \exp\{-i\pi\alpha_R(t)\}}{\sin\{\pi\alpha_R(t)\} \Gamma(\alpha_R(t))} \left(\frac{s}{Q^2}\right)^{\alpha_R(t)} \frac{\mu_U^2}{Q^2 + \mu_U^2} F_R^A(t), \end{aligned}$$

where  $\lambda_\gamma$  and  $\lambda_p$  are the helicities of the photon and the proton, respectively, and  $C_R^U = e_u - e_d$  for the ‘anomalous’  $f_1$  exchange and the ‘normal’  $f'_1$  Reggeon, while  $C_{a_1}^U = e_u + e_d$ . According to Eqs. (17)-(18), the central values of the parameters of the exchanges are:  $\alpha_{f_1}(t) = \alpha_{f_1}(0) = 0.88$ ,  $\beta_{f_1qq} \beta_{f_1NN} = -3.04$  GeV<sup>-2</sup>,  $\alpha_{f'_1}(t) = \alpha_{a_1}(t) = 0.622 + 0.9t$ ,  $\beta_{f'_1qq} \beta_{f'_1NN} = \frac{3}{5} \beta_{A_1qq} \beta_{A_1NN} = 13.57$  GeV<sup>-2</sup>,  $\mu_U = 1.45$  GeV.

The axial vector form factor in the Reggeon-nucleon vertex is given by [32]

$$F_R^A(t) = \frac{1}{(1 - t/1.17)^2}. \quad (24)$$

Only the transverse cross-section of  $\rho^0$  meson electroproduction is necessary to calculate double-spin asymmetries. As can be seen from Fig. 5, the model described above is in fair agreement with experimental data [33, 34].

It is, however, necessary to verify whether the assumption of  $s$ -channel helicity conservation is valid for the description of  $\rho^0$  electroproduction at HERMES. Otherwise, a large contribution from the spin-flip amplitude could exist which does not enter the matrix elements related to the structure functions and an important ingredient in the reaction mechanism could be lost. Experimentally [26] it was measured that the violation of SCHC is less than 10%.

Recently, HERMES has published data on a sizeable double-spin asymmetry in  $\rho^0$  meson electroproduction on the proton [35]. It is not expected that perturbative QCD calculations can explain this result, because for  $\rho^0$  production at HERMES energy there is no hard scale available. In general, pQCD calculations based on two gluon-exchange in the  $t$ -channel predict a very small asymmetry at  $t=0$  [36, 37]. The phenomenological Regge approach used here takes effectively into account non-perturbative effects of QCD which are important at HERMES energies.

The longitudinal double-spin asymmetry  $A_1^V$  for the interaction of transverse photons with a longitudinally polarized nucleon is defined as:

$$A_1^V(t) \equiv \frac{\sigma_T^{1/2} - \sigma_T^{3/2}}{\sigma_T^{1/2} + \sigma_T^{3/2}} = \frac{|M_T^{1/2}(t)|^2 - |M_T^{3/2}(t)|^2}{|M_T^{1/2}(t)|^2 + |M_T^{3/2}(t)|^2}. \quad (25)$$

Here  $M_T^{1/2}$  and  $M_T^{3/2}$  denote the transverse virtual photon scattering amplitudes where the superscript describes the projection of the total spin of the photon-nucleon system to the direction of the photon momentum. The amplitudes  $M_T^{1/2,3/2}$  contain spin-independent parts made up by exchanges with natural parity ( $M_N^{1/2,3/2}$ ) and spin-dependent parts made up by exchanges with unnatural parity ( $M_U^{1/2,3/2}$ ). Between them the following relations hold

$$M_N^{1/2}(t) = M_N^{3/2}(t), \quad M_U^{1/2}(t) = -M_U^{3/2}(t). \quad (26)$$

Then

$$\begin{aligned} A_1^V(t) &= 2 \frac{\text{Re}\{M_N^{1/2}(t)\} \text{Re}\{M_U^{1/2}(t)\}}{|M_N^{1/2}(t)|^2 + |M_U^{1/2}(t)|^2} + \\ &+ 2 \frac{\text{Im}\{M_N^{1/2}(t)\} \text{Im}\{M_U^{1/2}(t)\}}{|M_N^{1/2}(t)|^2 + |M_U^{1/2}(t)|^2}. \quad (27) \end{aligned}$$

At this point this asymmetry can be analyzed qualitatively. Both types of amplitudes contain real and imaginary parts. The sign of the imaginary part can be determined using the optical theorem, the sign of the real part follows from the Regge formula given in Eq. (1). The optical theorem reads

$$\sigma_{tot} = \frac{1}{s} \text{Im}\{M(s, 0)\}. \quad (28)$$

Since the total cross-section of photon-nucleon scattering is positive, the imaginary parts of the forward photon-nucleon scattering amplitude for Pomeron and  $f_2$  Reggeon exchanges are positive. It then follows from Eq. (1) that their real parts are negative. In the same way we deduce that the difference of imaginary parts of the photon-nucleon elastic scattering amplitude with anti-parallel and parallel spins  $\Delta M_U = M_U^{1/2} - M_U^{3/2} = 2M_U^{1/2}$

is positive if the contribution of the corresponding exchange to the structure function  $g_1(x, Q^2) \sim \sigma^{1/2} - \sigma^{3/2}$  is positive. The real part of  $\Delta M_U$  in this case is also positive. If the contribution to the spin structure function  $g_1(x, Q^2)$  is negative, the imaginary and real parts of the difference  $\Delta M_U$  are negative.

It is worthwhile to note that a direct estimate of the vector meson production asymmetry based on the relation  $A_1^V \approx 2A_1^{DIS}$  [38], even in the context of SCHC, does inherently not include the real part of the vector meson production amplitude as the DIS data on  $g_1$  and  $F_2$  are connected only to the imaginary part. For a full description, however, a way must be found to construct the real part which, in this paper, was chosen to be the Regge approach described above.

For the ‘anomalous’  $f_1$  exchange, the real part is much larger than the imaginary part and therefore this exchange should give a positive contribution to the asymmetry. For  $f_1'$  and  $a_1$  exchanges, real and imaginary parts of the amplitudes contribute with different signs to the asymmetry. For scattering on the proton, their real parts give a negative asymmetry, and the imaginary parts give a positive one. This is also the case for  $f_1'$  exchange when scattering on the neutron and on the deuteron. For  $a_1$  exchange in the case of scattering on the neutron, the real part of the amplitude leads to a positive double-spin asymmetry and the imaginary part leads to a negative one. Altogether, this discussion applies only to the region of small  $|t|$  where the corresponding amplitudes do not change sign ( $\alpha = 0$ ). Since the elastic cross-section originates mainly from the small  $|t|$  region, we expect this qualitative analysis to be valid.

The calculated predictions for double-spin asymmetries are shown in Figs. 6-13. Shaded areas were chosen to illustrate the range in the predictions obtained when different values for the ‘anomalous’  $f_1$  intercept are used. The upper limit of this range,  $0.74 - 0.93$  (cf. Eq. 17), is determined by the restriction that it is necessary to reproduce the transverse cross section shown in Fig. 5. Intercept values very close to unity are excluded, because otherwise the propagator in Eq. (1) would yield a too large contribution for  $\alpha_{f_1} \rightarrow 1$ .

From the figures it is evident that the contributions of the secondary  $f_1'$  and  $a_1$  Reggeons to the asymmetry are not small. At HERMES energies, they are of about the same size as the contribution of the ‘anomalous’  $f_1$  exchange which we considered previously [7] within another approach.

More information about the flavor composition of the asymmetry can be obtained when considering the case of the deuteron and the neutron. For the deuteron the isovector exchange contribution to  $A_1^V$  vanishes, and for the neutron it comes with the opposite sign and partly cancels the regular isoscalar part. By this reason the

‘anomalous’ part can be observed best when studying data on the neutron.

The dependencies of the double-spin asymmetry  $A_1^{\downarrow}$  on various kinematic variables are displayed in these figures for proton and deuteron. The Regge-based predictions were calculated for the HERMES kinematics,  $\langle W \rangle = 4.9$  GeV,  $\langle Q^2 \rangle = 1.7$  GeV<sup>2</sup>,  $\langle x \rangle = 0.07$ , and compared to measurements of  $\rho^0$  electroproduction at HERMES [35, 39, 40] on proton and deuteron. Although qualitative agreement can be seen only in the case of the proton, it is evident that experimental data with considerably improved precision are required.

## VI. CONCLUSIONS

In summary, the nucleon structure functions  $F_2(x, Q^2)$  and  $g_1(x, Q^2)$  were analyzed in the framework of a Regge approach. From the data on deep inelastic scattering on the proton, neutron and deuteron we derived the parameters of Reggeons with natural and unnatural parities in the region  $Q^2 = 1 \div 3$  GeV<sup>2</sup>. Using this parameterization and a non-relativistic model of  $\rho^0$  meson formation which provides a fair description of the cross-section, we calculated the double-spin asymmetry of  $\rho^0$  meson electroproduction at HERMES energies.

In this study we have used a unified approach to both DIS spin-dependent structure functions and vector meson electroproduction, in the context of  $s$ -channel helicity conservation. In this approach the obtained large value of the double-spin asymmetry in  $\rho^0$  meson production is correlated with the anomalous behavior of the flavor-singlet part of the structure function  $g_1(x, Q^2)$  at small  $x$ . In the case that future measurements will not confirm such a large asymmetry, for a Regge-type analysis it would have to be concluded that the ‘anomalous’  $f_1$  exchange is not a simple Regge pole but has a more complicated structure, e.g. a Regge cut.

## Acknowledgments

We are grateful to N.Bianchi, S.V.Goloskokov and O.V.Teryaev for useful discussions. This work was supported by the following grants RFBR-01-02-16431, INTAS-2000-366, EC-IHP-HPRN-CT-2000-00130, MCyT-BFM2001-0262, GV01-216, and by the Heisenberg-Landau program. A.V. thanks ICTP for the warm hospitality extended to him during his stay when a part of this work was completed and V.V. acknowledges the hospitality of Seoul National University during the last stages of this work.

---

[1] B. Adeva *et al.* [Spin Muon Collaboration], Phys. Rev. D **58**, 112001 (1998).

K. Abe *et al.* [E143 collaboration], Phys. Rev. D **58**,



- 112003 (1998).  
A. Airapetian *et al.* [HERMES Collaboration], Phys. Lett. B **442**, 484 (1998).  
P. L. Anthony *et al.* [E142 Collaboration], Phys. Rev. D **54**, 6620 (1996).  
K. Abe *et al.* [E154 Collaboration], Phys. Rev. Lett. **79**, 26 (1997).  
K. Ackerstaff *et al.* [HERMES Collaboration], Phys. Lett. B **404**, 383 (1997).
- [2] J. Bartels, B. I. Ermolaev and M. G. Ryskin, Z. Phys. C **72**, 627 (1996).  
[3] E. A. Kuraev, L. N. Lipatov and V. S. Fadin, Sov. Phys. JETP **45**, 199 (1977) [Zh. Eksp. Teor. Fiz. **72**, 377 (1977)].  
[4] V. S. Fadin and L. N. Lipatov, Phys. Lett. B **429**, 127 (1998).  
[5] N. I. Kochelev *et al.*, Phys. Rev. D **61**, 094008 (2000).  
[6] N. I. Kochelev *et al.*, Nucl. Phys. Proc. Suppl. **99A**, 24 (2001).  
[7] N. I. Kochelev, D. P. Min, V. Vento and A. V. Vinnikov, Phys. Rev. D **65**, 097504 (2002).  
[8] Y. Oh, N. I. Kochelev, D. P. Min, V. Vento and A. V. Vinnikov, Phys. Rev. D **62**, 017504 (2000).  
[9] P. D. Collins, "An Introduction To Regge Theory And High-Energy Physics," *Cambridge 1977, 445p.*  
[10] E. Levin, TAUP-2465-97, DESY-97-213, arXiv:hep-ph/9710546.  
[11] A. B. Kaidalov and Y. A. Simonov, Phys. Lett. B **477**, 163 (2000).  
[12] D. Kharzeev and E. Levin, Nucl. Phys. B **578**, 351 (2000).  
[13] E. V. Shuryak and I. Zahed, Phys. Rev. D **62**, 085014 (2000).  
[14] M. Guidal, J. M. Laget and M. Vanderhaeghen, Nucl. Phys. A **627**, 645 (1997).  
[15] S. I. Manaenkov, arXiv:hep-ph/9903405.  
[16] A. Donnachie and P. V. Landshoff, Phys. Lett. B **296**, 227 (1992).  
[17] D. E. Groom *et al.* [Particle Data Group Collaboration], Eur. Phys. J. C **15**, 1 (2000).  
[18] P. V. Landshoff and O. Nachtmann, Z. Phys. C **35**, 405 (1987).  
[19] A. Capella, A. Kaidalov, C. Merino and J. Tran Thanh Van, Phys. Lett. B **343**, 403 (1995).  
[20] C. Adloff *et al.* [H1 Collaboration], Phys. Lett. B **520**, 183 (2001).  
[21] J. Breitweg *et al.* [ZEUS Collaboration], Eur. Phys. J. C **7**, 609 (1999).  
[22] H. Abramowicz, E. M. Levin, A. Levy and U. Maor, Phys. Lett. B **269**, 465 (1991).  
A. Donnachie and P. V. Landshoff, Z. Phys. C **61**, 139 (1994).
- [23] M. R. Adams *et al.* [E665 Collaboration], Phys. Rev. D **54**, 3006 (1996).  
M. Arneodo *et al.* [New Muon Collaboration], Nucl. Phys. B **483**, 3 (1997).  
D. Allasia *et al.*, Z. Phys. C **28**, 321 (1985).  
S. Aid *et al.* [H1 Collaboration], Nucl. Phys. B **470**, 3 (1996).  
C. Adloff *et al.* [H1 Collaboration], Nucl. Phys. B **497**, 3 (1997).  
M. Derrick *et al.* [ZEUS Collaboration], Z. Phys. C **69**, 607 (1996).  
J. Breitweg *et al.* [ZEUS Collaboration], Eur. Phys. J. C **7**, 609 (1999).  
[24] J. Soffer and O. V. Teryaev, Phys. Rev. D **56**, 1549 (1997).  
S. D. Bass and M. M. Brisudova, Eur. Phys. J. A **4**, 251 (1999).  
[25] N. Bianchi and E. Thomas, Phys. Lett. B **450**, 439 (1999).  
[26] M. Tytgat, DESY-THESIS-2001-018.  
[27] L. Rosenberg, Phys. Rev. **129**, 2786 (1963).  
[28] M. Anselmino, A. Efremov and E. Leader, Phys. Rept. **261**, 1 (1995) [Erratum-ibid. **281**, 399 (1997)].  
[29] A. Donnachie and P. V. Landshoff, Phys. Lett. B **185**, 403 (1987).  
[30] J. M. Laget, Phys. Lett. B **489**, 313 (2000).  
[31] I. Royen and J. R. Cudell, Nucl. Phys. B **545**, 505 (1999).  
[32] A. Liesenfeld *et al.* [A1 Collaboration], Phys. Lett. B **468**, 20 (1999).  
[33] A. Airapetian *et al.* [HERMES Collaboration], Eur. Phys. J. C **17**, 389 (2000).  
[34] M. R. Adams *et al.* [E665 Collaboration], Z. Phys. C **74**, 237 (1997).  
[35] A. Airapetian *et al.* [HERMES Collaboration], Phys. Lett. B **513**, 301 (2001).  
[36] M. Vanttinen and L. Mankiewicz, Phys. Lett. B **440**, 157 (1998),  
M. Vanttinen and L. Mankiewicz, Phys. Lett. B **434**, 141 (1998).  
[37] S. V. Goloskokov, Eur. Phys. J. C **11**, 309 (1999).  
[38] H. Fraas, Nucl. Phys. B **113**, 532 (1976).  
N. N. Nikolaev, Nucl. Phys. Proc. Suppl. **79**, 343 (1999).  
[39] K. Lipka ( *for the HERMES Collaboration*), World Scientific, Proc. of PHOTON 2001, 186 (2002).  
[40] K. Lipka, talk at An International Conference on The Structure and Interactions of the Photon (PHOTON 2001), Ascona Switzerland September 2nd-7th 2001, <http://hep-proj-photon2001.web.cern.ch/hep-proj-photon2001/proc/proc.htm>

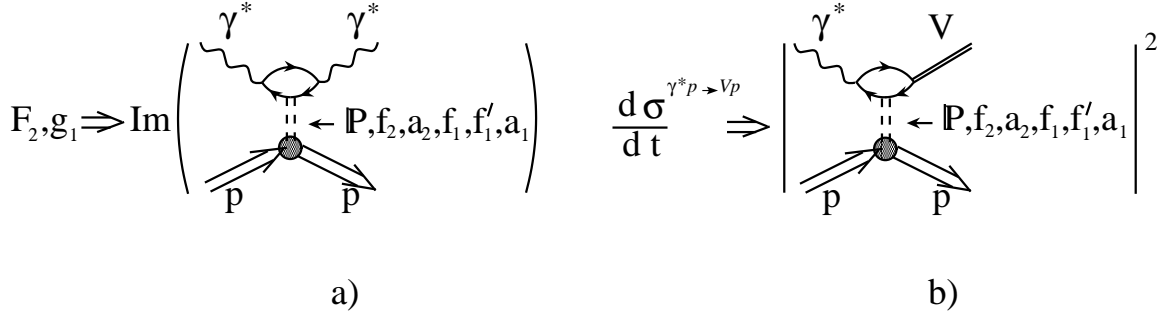


FIG. 1: S-channel helicity conservation implies that the same exchanges describe the structure functions ( $F_2$  and  $g_1$ ) of inclusive deep inelastic lepton scattering [panel a)] and of vector meson production processes at high energy [panel b)].

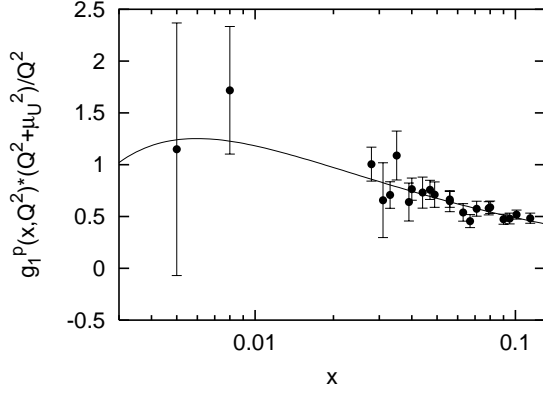


FIG. 2: The result of the fit of the proton structure function  $g_1(x, Q^2)$  in the Regge region ( $x < 0.1$ ) and at  $Q^2 = 1 - 3 \text{ GeV}^2$  in comparison with the data [1].

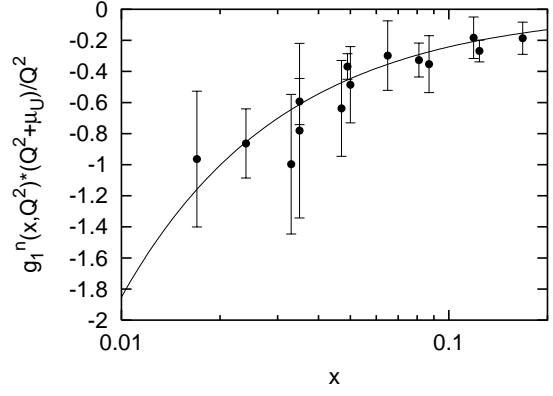


FIG. 3: The result of the fit of the neutron structure function  $g_1(x, Q^2)$  in the Regge region ( $x < 0.1$ ) and at  $Q^2 = 1 - 3 \text{ GeV}^2$  in comparison with the data [1].

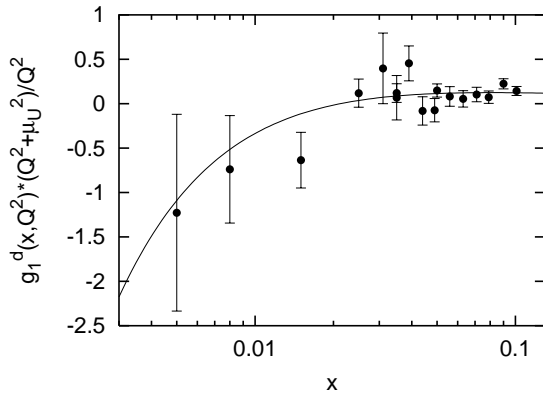


FIG. 4: The result of the fit of the deuteron structure function  $g_1(x, Q^2)$  in the Regge region ( $x < 0.1$ ) and at  $Q^2 = 1 - 3 \text{ GeV}^2$  in comparison with the data [1].

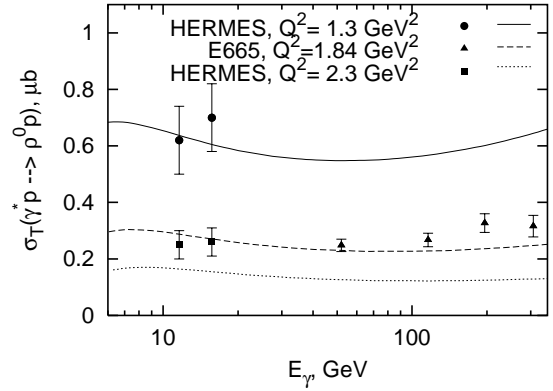


FIG. 5: The cross-section of  $\rho^0$  electroproduction by transverse photons is shown. The data points have been obtained from the published total and longitudinal cross-sections measured at HERMES [33] and E665 [34]. The solid, dashed and dotted lines represent the model calculations at the given  $Q^2$  values.

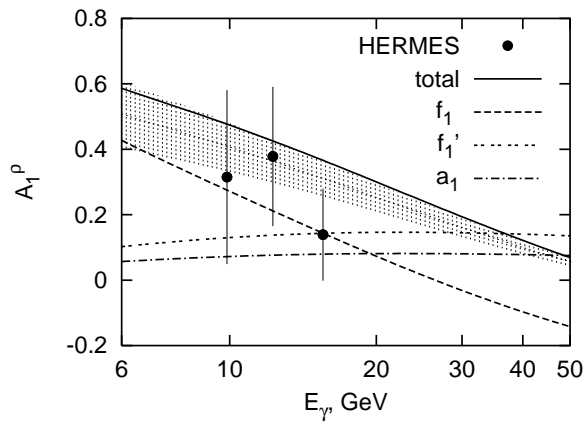


FIG. 6: The  $E_{\gamma^*}$ -dependence of the double-spin asymmetry  $A_1^p$  on the proton compared to data calculated from results of HERMES [35]. The shaded area corresponds to the interval of allowed values  $0.72 \div 0.93$  for the anomalous  $f_1$  intercept (see section V).

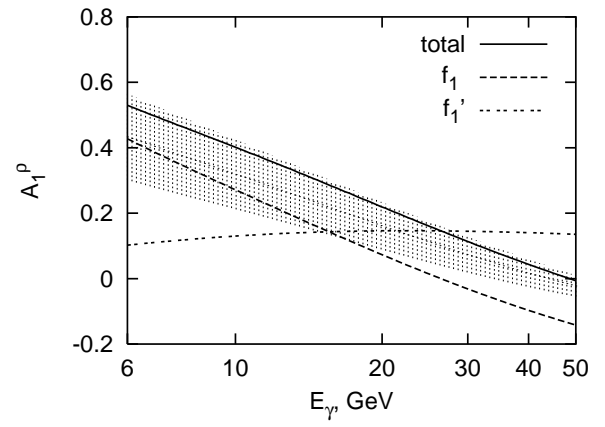


FIG. 7: The  $E_{\gamma^*}$ -dependence of the double-spin asymmetry  $A_1^p$  on the deuteron is shown. The notations are the same as in Fig. 6.

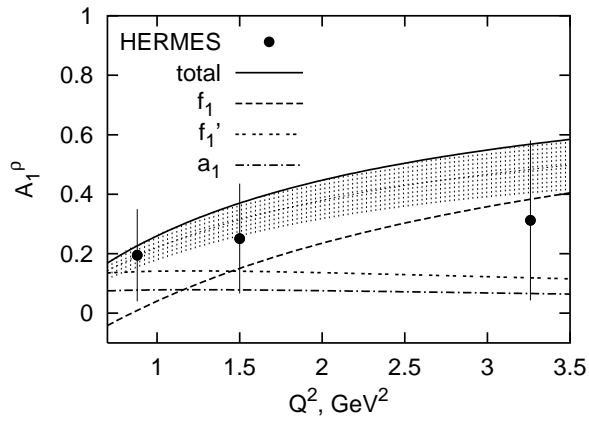


FIG. 8: The  $Q^2$ -dependence of the double-spin asymmetry  $A_1^p$  on the proton, compared to results of HERMES [35]. The notations are the same as in Fig. 6.

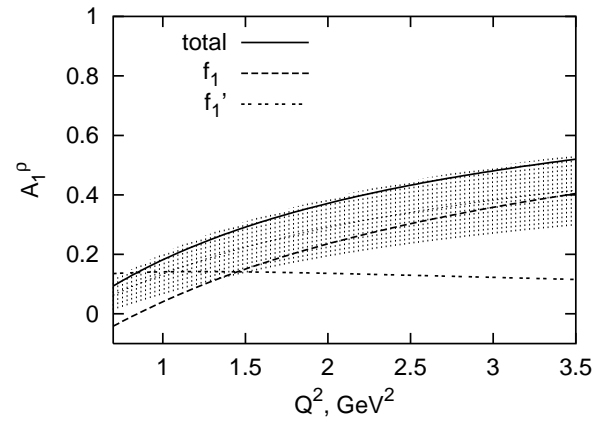


FIG. 9: The  $Q^2$ -dependence of the double-spin asymmetry  $A_1^p$  on the deuteron is shown. The notations are the same as in Fig. 6.

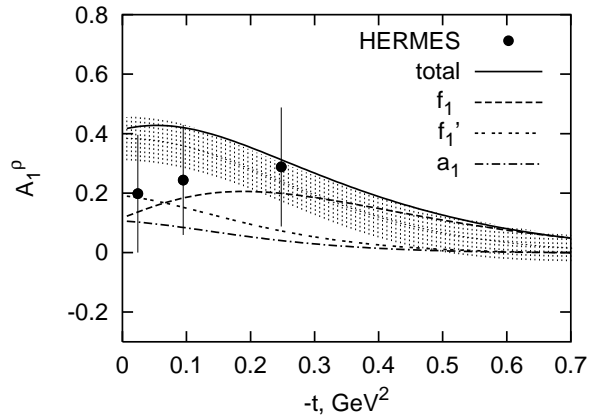


FIG. 10: The  $-t$ -dependence of the double-spin asymmetry  $A_1^p$  on the proton, compared to results of HERMES [35]. The notations are the same as in Fig. 6.

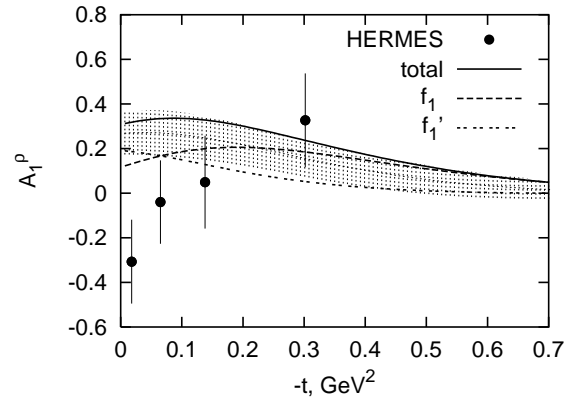


FIG. 11: The  $-t$ -dependence of the double-spin asymmetry  $A_1^p$  on the deuteron, compared to preliminary results of HERMES [40]. The notations are the same as in Fig. 6.

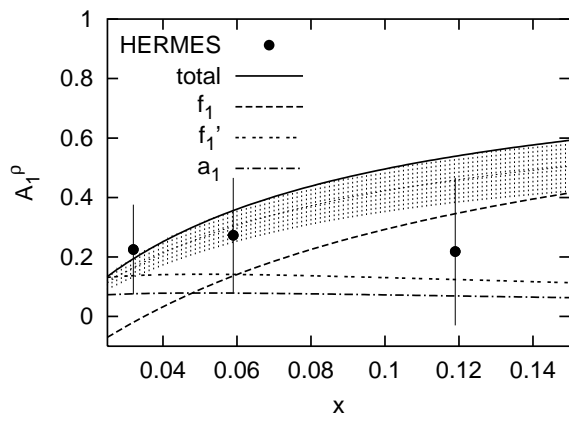


FIG. 12: The  $x$ -dependence of the double-spin asymmetry  $A_1^p$  on the proton, compared to results of HERMES [35]. The notations are the same as in Fig. 6.

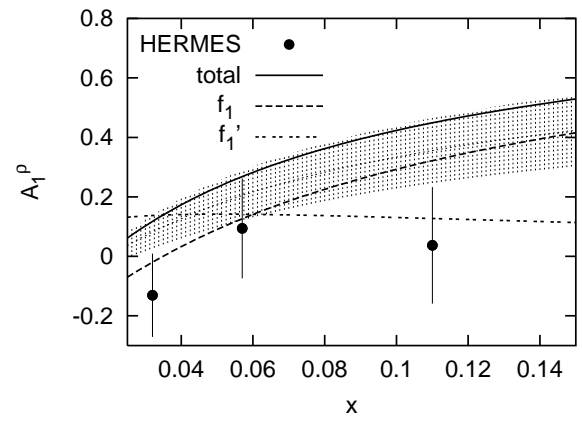


FIG. 13: The  $x$ -dependence of the double-spin asymmetry  $A_1^p$  on the deuteron, compared to preliminary results of HERMES [39]. The notations are the same as in Fig. 6.